

# We are IntechOpen, the world's leading publisher of Open Access books Built by scientists, for scientists

6,900

Open access books available

186,000

International authors and editors

200M

Downloads

Our authors are among the

154

Countries delivered to

TOP 1%

most cited scientists

12.2%

Contributors from top 500 universities



WEB OF SCIENCE™

Selection of our books indexed in the Book Citation Index  
in Web of Science™ Core Collection (BKCI)

Interested in publishing with us?  
Contact [book.department@intechopen.com](mailto:book.department@intechopen.com)

Numbers displayed above are based on latest data collected.  
For more information visit [www.intechopen.com](http://www.intechopen.com)



# NMR Spectroscopy for Studying Integrin Antagonists

Nathan S. Astrof<sup>1</sup> and Motomu Shimaoka<sup>2\*</sup>

<sup>1</sup>Mount Sinai School of Medicine

<sup>2</sup>Department of Molecular Pathobiology and Cell Adhesion Biology,  
Mie University Graduate School of Medicine  
Japan

## 1. Introduction

The expansion of the modern pharmacopeia is driven by advances in structural genomics that enable the detailed understanding of drug – protein interactions necessary for the identification of novel compounds as well as improved variants of existing drugs. Our research has centered on understanding the mechanism by which a critical class of transmembrane receptor proteins, the integrins, become activated in healthy and disease states. An important component of this research has been in identifying novel inhibitors of integrin function and their mechanism of action. As we describe in the following sections, nuclear magnetic resonance spectroscopy (NMR) has been an essential tool in advances in this area, and is the major focus of this review.

Integrins are a family of cell surface receptor proteins that mediate cell-matrix and cell-cell adhesion (Hynes, 2002). Integrin mediated adhesion is critical in multiple phases of development and maintenance of tissue physiology. Conversely, aberrant integrin function that can arise due to inappropriate increase or decrease in expression levels as well as inappropriate levels of activation is implicated in many diseases including cancer, neurological and immunological disorders (Shimaoka and Springer, 2003). The critical role of integrins in maintenance of healthy physiology has stimulated intense efforts to understand the mechanism of integrin mediated adhesion and identify pharmacological agents that can alter integrin function and thus restore the appropriate levels of cellular adhesion. Although the focus of this review is on NMR spectroscopy, as opposed to the related technique of magnetic resonance imaging (MRI), many of the compounds identified as integrin antagonists are also of interest as probes for MRI, particularly in the area of cancer imaging (Dijkgraaf et al., 2009). Thus, although we confine ourselves to understanding the interactions between antagonists and integrins by NMR *in vitro*, many of these results are directly applicable to the study of integrin expression and function by MRI *in vivo*.

Nuclear magnetic resonance (NMR) spectroscopy has played a central role in understanding the mechanism of integrin activation and providing insight into the nature and dynamic

---

\* Corresponding Author

consequences of known small molecule modulators of integrin function (Beglova et al., 2002; Kallen et al., 1999). However, integrins are large (~2 megadalton), poly-glycosylated, membrane-associated receptor proteins and NMR studies of systems of such complexity are exceptionally challenging. Fortunately, (at least some of) the ecto- domains of the integrin heterodimer can be expressed in the absence of the transmembrane segments and retain ligand binding function and specificity (Xiong et al., 2007). In particular, the ligand binding I-domain, is found in half of all vertebrate integrins and can be expressed (and isotope labeled) using conventional bacterial over-expression systems (Kriwacki et al., 2000; Lambert et al., 2008; Legge et al., 2000). Many potent integrin antagonists that target the I domain have been developed drawing on the structural insights of NMR investigations into I-domain : antagonist structure, and this remains an active and promising area of research (Constantine et al., 2006; Crump et al., 2004; Liu et al., 2001; Winn et al., 2001; Weitz-Schmidt et al., 2001).

Although there has been great progress in understanding integrin biology using recombinantly expressed fragments, there is also considerable interest in studying the regulation of integrin function *in situ*. Integrins are regulated by signals originating both outside and within the cell on which they are expressed and a pure *in vitro* system can-not fully recapitulate the complex dynamics of cellular signaling. The large size and transmembrane linkage limits the use of routine solution experiments for NMR observation of the integrin in the native environment. However, techniques described in this review, including saturation transfer difference NMR (STD-NMR), allow for a detailed investigation into the binding mechanism from the perspective of the ligand (Mayer and Meyer, 1999). Although the integrin is not directly observed in these techniques, these investigations bridge the gap between structural studies of integrin ligands in solution by NMR and high-resolution structures of integrins obtained both by crystallography and advanced modeling techniques (Wagstaff et al., 2010b; Claasen et al., 2005; Meinecke and Meyer, 2001). These methods are useful both in large scale screening programs and also to understand conformational changes in ligands associated with integrin binding.

## 2. Integrin function in physiology and disease

Integrins are a family of metazoan specific transmembrane proteins that mediate cell adhesion (intercellular and cell-matrix) and transmit signals associated with attachment into the cell (Hynes, 2002). Integrins are expressed on all cell types and have a panoply of physiological roles in development, as evidenced by the dramatic phenotype(s) observed in transgenic knock-out models of many integrins or their protein ligands e.g. (George et al., 1993; Yang et al., 1993). Some integrins, though less critical during development, are absolutely required for survival of the mature organism. For example, knockout of the leukocyte restricted integrin LFA-1 results in pronounced but selective immune deficits, underscoring the importance of LFA-1 in multiple phases of the immune response (Ding et al., 1999).

Integrins can rapidly up and down regulate their affinity for ligands from the basal to fully activated state (Shamri et al., 2005). This differs from other adhesion molecules that require changes in cell surface expression and in-membrane diffusion to modulate the adhesive properties of the cells on which they are expressed. Cells utilize the dynamic nature of integrin adhesion to dynamically modulate their interaction with the surrounding

environment on a timescale much shorter than possible with other cell adhesion molecules. Conversely, the dynamic nature of integrin-mediated adhesion requires a precision regulatory apparatus since even small perturbations in integrin activity regulation can have pronounced effects. This is strikingly evident in murine transgenics in which constitutively active variants are 'knocked-in' to replace the normal wild-type variants. These knock-in mice display phenotypes often as severe as the transgenic knock-out of the same gene (Imai et al., 2008; Park et al., 2007; Semmrich et al., 2005).

Each integrin is formed from the non-covalent association of 1 of 18 alpha subunits and 1 of 8 beta subunits with 24 known combinations expressed on mammalian cells excluding splice variants (Hynes, 2002). For example, the integrin LFA-1 is formed from the alphaL subunit and the beta2 subunit, designated  $\alpha_L\beta_2$ . A third commonly encountered nomenclature is the cluster of differentiation where LFA-1 is designated CD11a/CD18. The integrin Mac-1, found predominantly on neutrophils, is formed from the common beta2 (CD18) subunit but uses the CD11b alpha chain and is designated as  $\alpha_M\beta_2$  or CD11b/CD18. The complete array of mammalian integrins is shown in **FIGURE 1**.

Each integrin has a unique, but overlapping, ligand binding profile (Campbell and Humphries, 2011). Most integrin ligands are extracellular matrix molecules including fibronectin, vitronectin and collagen. Other ligands are cell surface proteins, such as the Intercellular Adhesion Molecules (ICAMs). A canonical recognition motif for many integrins is Arg-Gly-Asp (RGD), with residues flanking either end of the triplet responsible for specifying the correct conformation to bind to distinct integrins (Ruoslahti, 1996). Other integrins recognize unique motifs found in a select group of protein(s). While many integrins do not recognize the RGD motif, an acidic moiety is a common feature of all integrin ligands (Plow et al., 2000).

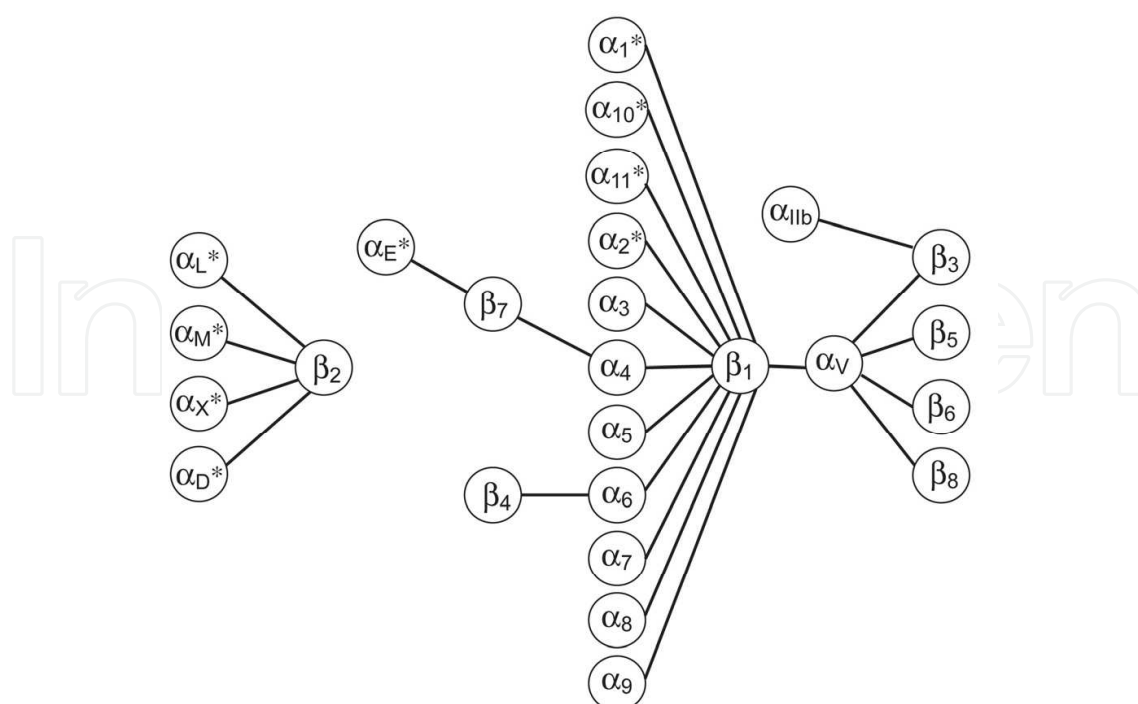


Fig. 1. Integrin subunit combinations. 18 alpha and 8 beta subunits form 24 integrin heterodimers. Asterisks denote alpha subunits containing an inserted (I) domain.

## 2.1 Disease

Integrins are involved in all aspects of mammalian physiology. It is not surprising that integrins are also involved in the pathogenesis of numerous diseases. Integrins involvement in disease initiation and progression may result either via direct perturbation of integrin expression or function. Alternatively, integrin function may be exploited to circumvent ordinary protection against disease physiology. One of the central challenges of pharmacology is to selectively alter integrin function that promotes the disease state in the much greater background of normal integrin activity (Shimaoka and Springer, 2003).

*Cancer:* Several Integrins play a crucial role in cancer development and the specific integrins varies depending upon the primary origin of the cancer (Jin and Varner, 2004). Down regulation of integrin expression is required to migrate to secondary tissues as well as establish a secondary site of growth. The high metabolic needs of cancer cells also requires extensive angiogenesis, the growth of blood vessels. Two  $\alpha$ V integrins ( $\alpha$ V $\beta$ 3 and  $\alpha$ V $\beta$ 8) have received considerable interest due to their role in cell survival and promoting angiogenesis (Nemeth et al., 2007). Appreciation of the critical role of these integrins in cancer has led to the development of inhibitors targeting  $\alpha$ V integrins as chemotherapeutics. One example, the cyclic RGD-f(NMet) peptide, is currently in clinical trials for glioblastoma (Reardon et al., 2008).

*Thrombosis:* Integrin  $\alpha$ IIb $\beta$ 3 binding to ligand fibrinogen is required for the process of blood clot formation. Aberrant clot formation is occurring within blood vessels is called thrombosis, a life-threatening condition (Coller and Shattil, 2008). Thrombosis may be treated with drugs such as eptifibatide, a cyclic peptide derived from a snake venom protein barbourin with a KGD sequence that acts as an  $\alpha$ IIb $\beta$ 3 competitive antagonist (Scarborough, 1999).

*Autoimmunity:* Integrins play multiple roles within the immune system including mediating migration to and from the source of infections, stabilizing contacts between immune cells, delivering key co-stimulatory signals required for immune cell development and function, as well as mediating opsonization of foreign organisms (Evans et al., 2009). Autoimmune disorders, including multiple sclerosis, psoriasis and colitis, involve physiological integrin function being co-opted by dysfunctional immune cells, facilitating the propagation of disease. Developing selective inhibitors of leukocyte expressed integrins, particularly the  $\beta$ 2 family and the  $\alpha$ 4 integrins is a major focus of anti-inflammatory effector research (Shimaoka and Springer, 2003).

*Infection:* Although integrin function is obligate for normal immune homeostasis, several integrins are also exploited for the establishment and maintenance of several diseases. Integrins act as receptors or co-receptors for several viruses, including paploma virus ( $\alpha$ 6 $\beta$ 4) (Yoon et al., 2001), rotavirus ( $\alpha$ 2 $\beta$ 1 and  $\alpha$ 4 $\beta$ 1) (Fleming et al., 2007), Ebola virus ( $\alpha$ 5 $\beta$ 1) (Schornberg et al., 2009) and adenoviruses (Cuzange et al., 1994). These interactions may be with the canonical ligand binding regions or with other regions of the integrins, a critical consideration in the design of selective inhibitors of pathogen – integrin interactions. Some integrins may also facilitate the formation of a virological synapse and promote the spread of lentiviruses such as HIV (Cicala et al., 2011).



### 3. Integrin structure

Both  $\alpha$  and  $\beta$  integrin subunits are complex, multidomain single-span type-I transmembrane glycoproteins with short (but critical) cytoplasmic sequences excluding  $\beta 4$  which has a large intracellular domain (**FIGURE 2A-C**). High-resolution structural techniques including x-ray crystallography, cryo-electron microscopy (cryo-EM) and NMR spectroscopy have converged on a model of the individual integrin domains and their role in the transition from inactive to active state. Of particular importance is the high level of sequence conservation within the integrin family, such as the location and number of critical disulphide bonds (Luo et al., 2007). Thus, although high-resolution structures have only been obtained for two intact members of the  $\beta 3$  family and a single  $\beta 2$  integrin, the structural insights gained are applicable to other integrins (Xie et al., 2004; Xiong et al., 2001).

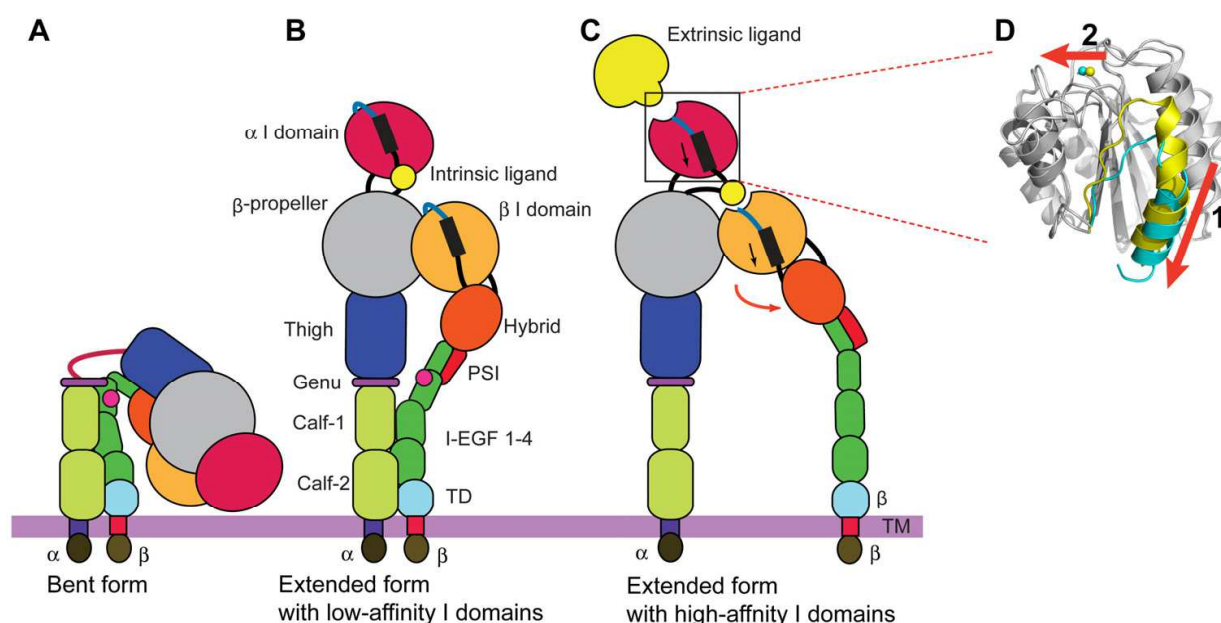


Fig. 2. Integrin structures and domains and conformational changes. (A-C) Global conformational changes between the bent (A), intermediate (B), and extended (C) conformations. Blow-ups showing the structures of the high- and low-affinity conformations of the alpha I domains (D). A piston-like downward shift of the C-terminal helix (arrow 1) is allosterically linked to the conversion of the MIDAS to the high-affinity configuration (arrow 2). Superposition of the high- (blue) and closed low- (yellow) affinity I domains is shown. Regions undergoing significant conformational changes are colored, whereas regions not undergoing significant conformational changes are in gray.

#### 3.1 Extracellular domain

##### 3.1.1 $\alpha$ -subunit

Integrin alpha subunits are organized in 4 or 5 domains and are approximately 1000 amino acids in length. The N-terminus forms a  $\beta$ -propeller with each strand of the propeller formed from a 4-stranded antiparallel  $\beta$ -sheet. C-terminal to the  $\beta$ -propeller is the thigh, calf-1 and calf-2 domains, all  $\beta$ -sandwich domains that bear topological similarity with

immunoglobulin domains. A short disulphide bonded loop, the genu, is positioned between the thigh and calf-1 domains; the genu can form a calcium coordinating site although this is not observed in all integrins (Xie et al., 2004). A furin protease cleavage site, located in calf-2 that separates the alpha subunit into light and heavy chains is found in a subset of integrins ( $\alpha 3$ ,  $\alpha 5$ ,  $\alpha 6$ ,  $\alpha 8$ ,  $\alpha V$ , and  $\alpha IIb$ ) (Campbell and Humphries, 2011).

In half of all mammalian integrin subunits ( $\alpha 1$ ,  $\alpha 2$ ,  $\alpha 10$ ,  $\alpha 11$ ,  $\alpha L$ ,  $\alpha X$ ,  $\alpha M$ ,  $\alpha D$ ,  $\alpha E$ ) an additional domain is inserted between blades 2 and 3 of the  $\beta$ -propeller. When present the Inserted (I-) domain forms all or part of the ligand-binding site (Shimaoka et al., 2002). Multiple crystal, and one NMR structure, have been determined of isolated I domains from several integrins. The I-domain is built from seven  $\alpha$ -helices wrapping five parallel and one anti-parallel strands that generally alternate in the protein sequence. On the 'top' face of the I domain, five amino acids side chains form a divalent cation binding site (the metal ion dependent adhesion site, MIDAS) (Lee et al., 1995b; Qu and Leahy, 1995). A ring of hydrophobic residues (the hydrophobic cup) surrounds the MIDAS site (Shimaoka et al., 2002). The N- and C- termini of the I domain are in close proximity and form flexible linkers to the  $\beta$ -propeller, as revealed in a recent crystal structure of the integrin  $\alpha X\beta 2$  (Xie et al., 2004).

The I domain from integrin  $\alpha M$  crystallizes in two conformations, termed open and closed (Lee et al., 1995a; Lee et al., 1995b). The two conformations, which are thought to represent endpoints of a conformational continuum, differ in the coordination sphere surrounding the MIDAS (**FIGURE 2D**). In the open conformation, one of the acidic residues coordinating the metal is replaced by a water molecule, the effect of which is to increase the electrophilicity of the metal. Since physiological integrin ligands contain acidic residues, reorganization of the MIDAS promotes ligand binding, as does the repositioning of loops on the top face that occurs in the open state. Also, in the open conformation the C-terminal helix is shifted downward by approximately two turns with respect to the position in the closed conformation. It is thought that conformational changes C-terminal helix acts as an allosteric switch regulating the conformation of the ligand binding face, a hypothesis that is supported by additional biochemical evidence and computer simulations (Jin et al., 2004; Xiong et al., 2000).

Unlike  $\alpha M$ , the I domain from  $\alpha L$  does not crystallize naturally in the open conformation; this is consistent with the observation that the isolated wild-type  $\alpha M$  I domain retains affinity for ligand while the I domain from  $\alpha L$  does not (Lu et al., 2001b; Qu and Leahy, 1995). However, using the open structure of  $\alpha M$  as a template, it has been possible to engineer disulphide bonds in the  $\alpha L$  sequence that stabilize the conformation of the open state (Lu et al., 2001a). Locking the  $\alpha L$  I domain in the open conformation results in a  $10^4$  increase in affinity for ligand. In a co-crystal of the high affinity  $\alpha L$  I domain with a two domain fragment of the ligand Intracellular Adhesion Molecule-1 (ICAM-1-D1D2), the C-terminal helix is found in the (expected) downward conformation and the ligand binding face, including the MIDAS, has undergone the appropriate conformational changes to facilitate binding to ligand. A number of polar and electrostatic interactions adjacent to the hydrophobic cup (and absent in  $\alpha M$ ) confer specificity of the I-domain : ICAM-1 interaction (Shimaoka et al., 2003).

### 3.1.2 $\beta$ -subunit

The  $\beta$  subunits are ~640 amino acids in length, organized into 8 discrete extracellular domains. The N-terminus is a 54 residue, 2 stranded antiparallel  $\beta$ -sheet linked by disulphide bonds to pair of short  $\alpha$  helices. The structure is homologous to the plexins and semaphorins and is thus called the Plexin-semaphorin-integrin (PSI) domain. Notably, the fourth disulphide bond is actually to a stretch of amino acids C-terminal to the adjacent hybrid domain, an immunoglobulin - like structure, such that the hybrid domain is inserted within the PSI domain (Luo et al., 2007).

Inserted within the hybrid domain is the  $\beta$ A or I - like domain, which is structurally homologous to the I-domain found in half of mammalian integrin  $\alpha$  subunits. The peculiar topology of the I-like domain, a domain inserted into a domain inserted into a domain, is critical for the mechanism of integrin activation. In addition to the MIDAS, there are two additional coordination sites whose occupancy regulates the affinity of the MIDAS metal for ligand through shared coordination residues. These two metal binding sites (the Adjacent to MIDAS, ADMIDAS, and Ligand Induced Binding Site, LIMBS) may also selectively directly coordinate some ligands (Xiao et al., 2004; Xiong et al., 2002).

The residues C-terminal to the I-like domain are organized into four- cysteine rich Epidermal Growth factor like (EGF) domains. The integrin-EGF (I-EGF) domains are highly homologous to the canonical domain but have additional numbers and/or placements of the disulphide bonds (Beglova et al., 2002; Takagi et al., 2001; Wouters et al., 2005). The most C-terminal ecto domain is the  $\beta$ -terminal domain ( $\beta$ TD), a novel fold with an N-terminal helix facing a mixed parallel/antiparallel  $\beta$ -strand.

*Transmembrane:* The transmembrane (TM) domains of integrins form a critical nexus between the extracellular and intracellular domains. Despite the great importance of the domains to the mechanism of integrin mediated adhesion and signaling, they are the least well-understood domains of integrin heterodimers. NMR of isolated transmembrane domains (in detergent solutions), disulphide cross-linking studies and molecular modeling studies have been used to identify the interface between the two chains. These studies converge on a right-handed coil-coil structure, which persists into the cytoplasm, similar to the previously determined structure of the TM protein glycophorin (Gottschalk, 2005; Li et al., 2002; Luo et al., 2004).

*Cytoplasmic:* Integrin cytoplasmic domains play a role in integrin function that is disproportionate to their generally small size. Interactions between the  $\alpha$  and  $\beta$  cytoplasmic domains help constrain integrins in the inactive conformation (Vinogradova et al., 2002). Phosphorylation of the cytoplasmic domains regulates indirect interactions with the cytoskeleton and protein signaling complexes (Fagerholm et al., 2004). The cytoplasmic tail complexes of two integrins,  $\alpha$ IIb $\beta$ 3 and  $\alpha$ L $\beta$ 2 have been extensively studied by NMR (Vinogradova et al., 2002). The  $\alpha$ IIb tail forms a short N-terminal a helix followed by a turn and a C-terminal loop that collapse back onto the N-terminal helix. The  $\beta$ 3 tail also forms an N-terminal helix while the majority of the tail lacks persistent structure. A salt bridge between residue arginine 995 in the  $\alpha$ IIb chain ( $\alpha$ R-995) forms with the aspartic acid 723 in the  $\beta$ 3 tail ( $\beta$ D-723). Prior biochemical studies of integrins using heterologous expression suggested the existence of a stabilizing salt bridge interaction as a critical element in



regulating the affinity state of integrins (Lu et al., 2001c). Notably, the cytoplasmic tail structure of the integrin  $\alpha\text{L}\beta 2$ , also determined by NMR, is significantly different (Bhunia et al., 2009). The  $\alpha\text{L}$  folds into three defined  $\alpha$ -helical segments with compact tertiary structure and the  $\beta 2$  tail into a single helix followed by unstructured segments. Like the  $\alpha\text{IIb}\beta 3$  tail complex, the  $\alpha\text{L}\beta 2$  association incorporates a prominent electrostatic interaction. Both similarities and differences in the two structures highlight the strengths, but also limitations, of extrapolating limited structural studies of one integrin to another, particularly in regions of lower sequence homology such as the tail domains.

#### 4. Architecture and activation mechanism

Overall, in both  $\alpha$  and  $\beta$  chains the integrin architecture can be divided into distinct structural elements. The integrin “head”, which includes the canonical ligand-binding site, is formed from the  $\beta$ -propeller in the  $\alpha$ -subunit and the I-like domain in the  $\beta$ -subunit. In a subset of integrins, the Inserted (I-) domain is also present in the integrin head. The headpiece includes both the head domains as well as the thigh domain in the  $\alpha$  chain and the plexin-semaphorin-integrin (PSI), and hybrid domains in the  $\beta$  subunit. The tailpiece is formed in the alpha subunit by the calf -1 and calf-2 domains and 4 integrin-type epidermal growth factor like (I-EGF) domains in the  $\beta$  subunit. The tailpiece is connected to the transmembrane domains which each span the membrane a single time and the (generally) short cytoplasmic sequences.

In the crystal structure of  $\alpha\text{V}\beta 3$ , the integrin is folded into a ‘V’ shape; a 135 degree angle is found between the head and tailpiece domains with a bend between the thigh and calf-1 domains in the alpha subunit and the I-EGF-1 and I-EGF-2 in the beta subunit. Although neither the transmembrane, nor the cytoplasmic domains are present in the crystallized proteins, they are generally regarded as being fully associated in the conformation visualized in the crystal structure. In this conformation, which establishes substantial inter and intradomain buried interfaces, the ligand-binding headpiece is inaccessible to ligands on opposing surfaces (Xiong et al., 2001).

Integrins that lack I-domains use an interface between the  $\beta$ -propeller and the I-like domain to form the ligand-binding site. The architecture of a canonical ligand binding motif was first identified in a crystal structure of the integrin  $\alpha\text{V}\beta 3$  with P5, a RGD containing cyclic peptide [Arg-Gly-Asp-{D-Phe}-N-methyl-Val] (Xiong et al., 2002). P5 binds within a crevice formed from the  $\beta$ -propeller and the  $\beta\text{A}$  domain; 335 Å, or 45% of the peptide surface area, is buried within the crevice. In the bound structure, the arginine and aspartic acid are pointed in opposite directions, the (partially solvent exposed) Arg pointing towards the  $\beta$ -propeller, inserted into a narrow sub-groove where it is stabilized by a pair of aspartic acids that form a bidentate salt bridge. The Asp is fully buried with one of the carboxylates coordinating the MIDAS metal; the second oxygen establishes a network of polar interactions with backbone amides and the aliphatic side chain makes additional hydrophobic contacts with protein side chain. The medial glycine sits at the  $\alpha/\beta$  interface, making hydrophobic contacts with the  $\alpha$  chain. Both of the non-RGD residues are purely structural, establishing the correct disposition of the RGD and point away from the  $\alpha/\beta$  interface.

The crystal structure of ligand bound integrins reveal a number of structural changes in the  $\beta$  chain I-like domain that are analogous to those that occur during activation of the I

domain. The  $\beta 6$ - $\alpha 7$  loop is repositioned and the C-terminal helix is shifted downward in a piston like motion. Subsequent structures reveal how ligand binding is coupled to activation of the holoreceptor (Xiao et al., 2004). Ligand binding to the  $\alpha II\beta 3$  headpiece crystal structure shows a profound swing out motion of the hybrid domain/PSI, away from the  $\alpha/\beta$  interface where the hybrid domain is tucked in the resting conformation. This motion propagates changes in the ligand-binding headpiece to the remainder of the integrin, and is a critical element of the *switchblade model* of integrin activation.

The switchblade model of integrin activation states that the integrin is in a conformational equilibrium between the bent state, observed in the crystal structure of  $\alpha V\beta 3$  and an extended conformation (or conformations) in which legs become separated and the headpiece becomes extended over the tailpiece (Luo et al., 2007). In this extended conformation, the headpiece is well disposed to bind ligands in the extracellular matrix or on the surface of opposing cells. Extension also favors dissociation of the transmembrane and cytoplasmic, facilitating the formation of signaling complexes on the tails. Integrin activation is bidirectional and can be driven either by ligand binding to the headpiece, favoring a swung out hybrid domain which in turn disrupts the stabilizing interfaces and favors receptor extension. Alternatively, activation may occur within the cell via binding of transiently exposed cytoplasmic tails which, stabilized in the dissociated conformation, can initiate conformational changes that propagate across the membrane, resulting in extension, swing out of the hybrid domain and an integrin primed for ligand binding.

In integrins that have an I domain in the  $\alpha$  subunit (i.e.  $\alpha L\beta 2$ ), there is a conserved acidic residue in the linker connecting the C-terminal tail back into the  $\beta$ -propeller (Alonso et al., 2002). When the C-terminal helix is shifted downward, the acidic residue can coordinate the  $\beta$  subunit MIDAS metal. The downward motion of the C-terminal helix thus transmits the effect of ligand binding to the I domain across the  $\alpha/\beta$  subunit interface with the acidic residue acting as an internal ligand. The subsequent steps of integrin activation are identical for both classes of integrins (Nishida et al., 2006).

## 5. NMR overview

NMR spectroscopy is an extensively used tool for the structural and dynamic characterization of proteins, small molecule ligands and their complexes. An exhaustive review of NMR theory and methodology is available in many organic and biological chemistry texts (e.g. (Cavanagh et al., 2006; Ege, 2003)); here, we selectively present information salient for understanding (and interpreting) published and future work on integrin and integrin – antagonist complexes.

NMR spectroscopy draws on quantum mechanical property of spin, the polarization of a subset of nuclear isotopes when placed in a magnetic field. This includes all three isotopes of hydrogen, the most abundant element in biomolecules. However, only the spin  $\frac{1}{2}$  nuclei – such as the  $^1\text{H}$  (proton) nucleus is commonly studied by NMR.  $^2\text{H}$  (deuterium) is a spin 1 nucleus; nuclei with spin  $>1/2$  are generally low sensitivity and difficult to observe in solution. The radioactive  $^3\text{H}$  (tritium) nucleus is not commonly observed, despite being spin  $\frac{1}{2}$  and the most sensitive NMR active nucleus. Fortunately, both carbon ( $^{13}\text{C}$ ) and nitrogen ( $^{15}\text{N}$ ) have a spin  $\frac{1}{2}$  isotope, albeit at low natural abundance ( $\sim 1\%$  and  $\sim 0.4\%$  respectively). To utilize these nuclei for biomolecular investigations it is necessary, in general, to increase

the enrichment levels. This can be accomplished by expressing proteins in organisms, typically *Escherichia coli*, that can grow in defined media containing appropriate isotopic precursors (i.e.  $^{15}\text{N}$  labeled ammonium chloride,  $^{13}\text{C}$  labeled glucose). Unfortunately, there is no spin  $\frac{1}{2}$  nucleus of oxygen, precluding direct observation in proteins and studies of hydrogen bonding in protein – ligand studies.

NMR experiments involve the perturbation of the equilibrium spin state by one or more appropriately tuned radio-frequency pulses and interspersed delay periods. This collection of pulses and delays is called a pulse sequence. A pulse sequence may be as simple as a single pulse applied to a single nucleus or involve hundreds of pulses and delays applied to as many as four nuclei. In both extremes, the resulting spectra (derived as the Fourier transform of the time dependent signal obtained by the NMR detector) are determined by the same set of three interactions: (1) chemical shift, (2) scalar (J-coupling) and (3) dipolar coupling that modulate the energy levels of the nuclear spins during the NMR experiment.

Local variations in electronic structure within the molecule result in the nucleus becoming more or less shielded from the spectrometer magnetic field, giving rise to small differences in nuclear magnetic energy levels. This phenomenon is known as the chemical shift and is the most readily observed effect in the NMR spectrum. Each peak in the NMR spectrum corresponds to the single type of nucleus in the molecule. Because each nucleus has a distinctive chemical shift, it is possible to obtain site-specific information throughout the molecule with the chemical shift of a particular nucleus acting as its molecular signature.

The J- coupling is an interaction between (directly or indirectly) covalently bonded NMR active nuclei. In the simple, one dimensional (1D) NMR experiment, the J-coupling between NMR active nuclei results in the NMR signals (peaks) to be split into multiple peaks. The number of peaks in the observed NMR spectrum is governed by the total number of coupled nuclei – each spin  $\frac{1}{2}$  nucleus coupled to  $n$  nuclei is split into  $n+1$  peaks. The magnitude of the J coupling is determined by: (a) the chemical nature of the coupled nuclei (heteronuclear vs. homonuclear), the number of covalent bonds between coupled nuclei and the relative orientation between the two coupled nuclei.

Finally, the dipolar coupling between nuclei is a through space interaction that depends on the distance between the two NMR active nuclei, as opposed to covalent connectivity. In simple NMR experiments, the dipolar coupling largely contributes to the line width of the peaks in the spectrum, since each NMR active nucleus acts as its own magnet and thus perturbs the magnetic field of those nuclei around it. The dipolar coupling gives rise to the Nuclear Overhauser effect (NOE), the perturbation of the energy state of one spin by another through space.

With simple organic molecules, it is possible to determine the molecular structure using one-pulse (i.e.  $^1\text{H}$  and  $^{13}\text{C}$ ) NMR experiments. Most organic groups have defined chemical shift ranges and, in conjunction with other spectroscopic techniques, the chemical shift and J-coupling provide suitable information to determine the molecular structure. For more complicated molecules – and especially large biopolymers, the enormous number of nuclei results in a complex, highly degenerate and uninterpretable NMR spectrum. The general approach to obtain resonance assignments for complex molecules is based upon a technique known alternatively as correlation or multidimensional NMR spectroscopy (nD NMR). In nD NMR, the NMR interactions, obtained by a suitably designed pulse sequence are

displayed along two ( $n = 2$ ) or more orthogonal axis. For example, the chemical shifts of two J-coupled nuclei can be obtained by an NMR experiment that first detects the chemical shift of the first nucleus, then allows for transfer between the two nuclei by the J coupling and then finally detects the chemical shift of the second nucleus. Alternatively, the same experiment can be performed by with transfer arranged via the NOE effect. Then, the chemical shifts of all nuclei close in physical space, but not necessarily covalently connected, can be obtained. Together, these techniques permit both the assignment of complex organic molecules as well as a determination of three- dimensional structure.

For moderately sized proteins ( $\leq 100$  amino acids), homonuclear (2D)  $^1\text{H}$ -NMR spectroscopy provides sufficient information to obtain resonance assignments, secondary and tertiary structural constraints suitable for the determination of high-resolution structure (Wuthrich, 1986). The resonance assignments phase proceeds in two steps. First, individual amino acids are assigned using J-coupling experiments to identify coupled sets of spins (spin systems), taking advantage of the characteristic proton fingerprint spin topologies of the natural amino acids. As there are no strong proton J-couplings between adjacent amino acid, this results in exclusively intra-residue assignments. Inter-residue connectivities are obtained via through space NOE experiments that allow correlations between protons that are close in space (i.e. on adjacent amino acids) but which are not necessarily detectably J-coupled.

2D- $^1\text{H}$  spectra of protein encode both distance and angle restraints that can be extracted from the spectra. The magnitudes of multi-bond scalar couplings (i.e. the three bond J coupling along the peptide backbone between the alpha and amide protons,  $^3J_{\text{C}\alpha\text{H}-\text{NH}}$ ) are a function of the intervening angles. The intensity of the cross peaks in  $^1\text{H}$ -NOE type experiments are proportional to the inverse sixth power of the distance between the two nuclei. Additional structural information is available from the pattern of chemical shifts that deviate in a regular pattern from that of an unstructured peptide depending upon the type of secondary structural element they are found in. Furthermore, during the NMR experiment, amide protons from the protein backbone can exchange with solvent if not protected by stable hydrogen bond formation. If deuterated water is used during the NMR experiment, hydrogens that have undergone exchange disappear from the spectrum. Thus, by dissolving the protein in  $^2\text{H}_2\text{O}$ , it is possible to identify amino acids that are located in regions of stable secondary structure, since they are protected from exchange with  $^2\text{H}$ . The data obtained can then be used to compute a family of NMR structures that satisfy the measured constraints.

The greater number of resonances, and higher molecular weight of larger proteins (which results in broader and less well resolved NMR signals) necessitates the use of heteronuclear ( $^{13}\text{C}$  and  $^{15}\text{N}$ ) multidimensional ( $n\text{D} > 2$ ) spectroscopy for resonance assignments and structure to be obtained. Numerous pulse sequences have been developed to obtain chemical shifts, scalar couplings and distances using the  $^{15}\text{N}$  and  $^{13}\text{C}$  chemical shifts to provide additional resolution for the spectra. Despite the additional complexity associated with performing these experiments (including the need to prepare isotopically labeled protein samples), the basic building blocks of structure determination are essentially the same as described for homonuclear  $^1\text{H}$  protein spectroscopy: obtain resonance assignments from intra- and inter-residue correlations, determine distance and spatial (angular) constraints, incorporate additional parameters such as amide protection and patterns of chemical shifts and convert experimental constraints into energy terms for computational refinement.



NMR experiments involve the perturbation of the collection of spins from their equilibrium, a process that is opposed by relaxation effects that restore the collection of spins back to their equilibrium state. Although spontaneous relaxation is an inefficient process, the motion of the protein in solution (both overall tumbling and low barrier transitions) gives rise to local magnetic fields that can result in the loss of the NMR signal. In general, there are two relaxation processes that are of interest.  $T_1$  (transverse) relaxation is the true relaxation of the spins to equilibrium state.  $T_2$  (longitudinal) relaxation is the loss of NMR coherence between two otherwise identical spins in different molecules. Both are a result of global and internal protein motions and place limits on the length (and complexity) of a given NMR experiment. While great care can be taken to minimize the effects on the NMR spectra (such as designing the shortest possible pulse sequences necessary to obtain required information) the relaxation processes also provide valuable information both on the overall shape of the protein (from tumbling effects) or internal conformational transitions (dynamics). The latter information is of increasing importance as it is recognized that proteins, rather than being static entities, exist in multiple inter-converting sub-states and that agonists and antagonist may function by favoring (or disfavoring) one or more of these states. Site specific information on protein dynamics is thus of both basic interest to understanding protein function but also of practical interest to the design of improved pharmaceuticals.

NMR experiments specifically designed to measure protein dynamics have been developed (Mittermaier and Kay, 2006). These include the aforementioned amide proton protection experiments, since transient opening of the protein structure permits the exchange of  $^1\text{H}$  with  $^2\text{H}$  which can be directly measured in a 2D  $^1\text{H},^{15}\text{N}$  J-coupling correlation experiment (the heteronuclear single quantum coherence, HSQC experiment) for each amide nucleus in the protein backbone and some side chains as well. More quantitative information on backbone protein dynamics can be obtained by measuring the  $T_1$  and  $T_2$ , as well as the  $^1\text{H}-^{15}\text{N}$  NOE. Methods have been developed to interpret these parameters in terms of the angular fluctuations and timescales of motion of the protein backbone. Similar experiments have been developed to monitor the dynamics of protein side chains using heteronuclear relaxation of isotopically labeled side chains.

Motions slower than that contributing to nuclear relaxation are also apparent in the NMR spectrum of proteins. For example, if the protein inter-converts between two or more conformations slower than the NMR data is recorded; two sets of resonances will appear in the spectrum. When this chemical exchange is faster, a single set of resonances may appear but the exchange parameters may be extracted from appropriately designed NMR experiments. Because these experiments measure biologically relevant timescale motions ( $\mu\text{s}$ - $\text{ms}$ ) they are of special interest in understanding protein function, and its perturbation by ligand binding (Palmer and Massi, 2006).

NMR dynamics and exchange experiments are excellent examples of NMR investigations where high-resolution structure determination is not necessarily the key endpoint. Other examples include measuring one or more NMR parameters, such as protein  $^1\text{H}$  and  $^{15}\text{N}$  chemical shifts in an HSQC experiment as a function of ligand concentration to identify binding sites (and in some cases binding constants). These experiments are particularly valuable when structure of the biomacromolecule of interest has already been obtained and the goal is restricted to identifying novel ligands, ligand variants or the mode of ligand binding. This approach, namely measuring a subset of crucial NMR parameters and



utilizing previously available information on the structure of the target molecule, is employed by many of the studies summarized in this review.

## 6. NMR of integrin I domain antagonists

The I domain from integrin LFA-1 has been the primary objective of numerous investigations to identify novel integrin antagonists. This is due both to the critical role of LFA-1 in mediating multiple phases of the immune response, as well as the capacity to produce large quantities of pure, soluble isotopically labeled protein to exploit the full range of tools of structural biology. An NMR structure of the  $\alpha$ L I domain was obtained using assignment and structural determination methods described in the prior section (Legge et al., 2000). In general, the topology is identical to that determined by x-ray crystallography. Most significantly, the C-terminal helix ( $\alpha 7$ ), which shows the greatest variation in crystallographic structures, is highly flexible, as determined both by absence of long-range  $^1\text{H}$ - $^1\text{H}$  NOEs, weak  $^1\text{H}$ - $^{15}\text{N}$  NOEs as well as limited protection against amide proton exchange, compared to the core of the protein. These observations validate the biophysical model and computer simulations of a flexible C-terminus acting as a ratchet or switch regulating the conformation and ligand binding activity of the protein (Jin et al., 2004).

The ligand for  $\alpha\text{L}\beta 2$  is the five-domain cell surface molecule Intracellular Adhesion Molecule (ICAM)-1. Titration of a soluble two domain ICAM-1 fragment (sICAM-1-D1-D2) into the protein labeled with  $^{15}\text{N}$  and / or  $^{15}\text{N}$ ,  $^{13}\text{C}$  revealed unique, concentration dependent behavior of the pattern of heteronuclear and proton chemical shifts (Huth et al., 2000). At high concentrations of ligand, extensive broadening in the NMR spectrum was observed, consistent with formation of a high molecular weight complex. At sub-saturating concentrations, however, the broadened residues were largely confined to two regions of the protein. Line broadening at residues around the MIDAS could be expected due direct chemical exchange with ligands. A second region of greater than average broadening was observed in the C-terminal helix and the opposing  $\beta$ -strand. The cleft between the two secondary structural elements was termed the I domain activation site (IDAS) as the basal and inducible ligand binding activity of several holoreceptors bearing mutations in the cleft was enhanced when compared to wild-type LFA-1 receptors.

### 6.1 Lovastatin

The allosteric regulation of I domain function by residues in the MIDAS suggests that some anti-LFA-1 antagonists may work via an allosteric mode of pharmacological intervention distinct from competitive inhibition. A high-throughput screen for small molecule antagonists of LFA-1 identified one such compound, lovastatin, which is the prototypical member of a class of small molecule allosteric integrin antagonists (Kallen et al., 1999).

Lovastatin, a fungal metabolite was earlier identified as competitive inhibitor of a 3-hydroxy-3'-methyl glutaryl coenzyme A (HMG CoA) reductase, an enzyme in the cholesterol biosynthetic pathway and is used clinically for the reduction of high serum cholesterol. However, lovastatin also has (potentially) beneficial immunosuppressive properties that may be independent of the role in lowering serum cholesterol. Together, the observation of immune-modulation properties of lovastatin and its identification in a screen

for LFA-1 antagonists suggests that the novel effects may be obtained directly via inhibition of LFA-1 (Weitz-Schmidt et al., 2001).

Using a cell based assay, lovastatin inhibits the adhesion of LFA-1 expressing cells to ICAM-1 substrate with an  $IC_{50} \sim 25 \mu M$ . Using a cell free assay with purified receptor and ligand proteins, the  $IC_{50}$  obtained was  $\sim 2.5 \mu M$ , demonstrating that the inhibition is a property of the proteins and does not involve the HMG-CoA reductase activity. Because lovastatin contains a lactone moiety that may be prone to hydrolysis, it was hypothesized that direct coordination of lovastatin acid to the MIDAS as the mechanism of inhibiting LFA-1 / ICAM-1 adhesion. Contrary to this suggestion, the hydroxyacid has weaker inhibition potential ( $>100 \mu M$  and  $\sim 14 \mu M$  for the cell based and cell free assays, respectively).

The mechanism of lovastatin inhibition of LFA-1 was directly addressing using soluble I domain labeled with  $^{15}N$  using an *E. coli* expression system (Kallen et al., 1999).  $^1H,^{15}N$  HSQC spectra were obtained for the free protein and in the presence of increasing concentrations of lovastatin-lactone or lovastatin-hydroxyacid. When the chemical shift differences between the free and drug added forms are mapped onto the structure of the I domain, a clear pattern became evident. The most significant perturbation in chemical shifts both in intensity and position are in the crevice between the C-terminal helix and the opposing beta sheet. Computer simulations further support the conjecture that lovastatin, and its derivatives, act as allosteric antagonists of LFA-1 function, preventing the obligate downward motion of the C-terminal helix (Gaillard et al., 2007).

A family of related statin derivatives was subsequently screened for binding to the I domain using a  $^1H,^{15}N$  - HSQC. By obtaining spectra as a function of ligand concentration (with fixed protein) it is possible to estimate the binding dissociation constant ( $K_D$ ) between statin derivative and I domain. The  $K_D$ s range from  $\sim 2.0 \mu M$  for lovastatin and simvastatin to  $\sim 8 \mu M$  for mevastatin. Prevastatin, with a hydroxylated terpenoid ring has an  $K_D > 100 \mu M$ , presumably due to the energetic costs of burying a polar residue in the largely hydrophobic crevice. The tightest binding inhibitor identified by NMR in this study was the synthetic derivative LFA703, which bound with  $\sim 0.2 \mu M$  affinity. Most significantly, these changes in  $K_D$  directly parallel the  $IC_{50}$  measured in using the intact holoreceptor in cell based assays, demonstrating that the I domain is the principle, and likely exclusive, source of the inhibitory effect and that screening allosteric antagonists by binding to isolated I domains is a valid approach to determining the affinity, and indirectly the efficacy, of I domain allosteric antagonists. Also, although the dynamics of the I -domain / lovastatin complex was not quantitatively measured, the spectra all showed signs of conformational exchange, consistent with fast binding and release kinetics of lovastatin or its derivatives from the I domain.

The demonstration of potent allosteric inhibition of the I domain has driven additional screens for LFA-1 antagonists derived from alternative chemotypes. One successful cell based screen identified a diaryl sulphide with an  $IC_{50}$  of  $\sim 2.3 \mu M$ , comparable to lovastatin (Crump et al., 2004). The addition of drug to  $^1H,^{15}N$  labeled protein results in chemical shift and intensity changes in the spectra (due to chemical exchange) that were analogous to those for lovastatin, demonstrating that the two dissimilar chemotypes utilized a common mechanism for inhibition of function. Additional synthetic diaryl sulfides were prepared

and also shown to bind to the same position of the I domain, albeit with dramatically greater efficacy (IC<sub>50</sub> ~44 nM). Unlike lovastatin and the parent compound, however, no chemical exchange broadening was observed in the spectrum, consistent with tighter binding of the derivative; this indicates that the improved efficacy is a function of better binding to the I domain, as opposed to acting on a second site on the intact receptor.

Although the HSQC spectra are a rapid means of identifying and characterizing compounds that bind to the I domain, the process of drug design is greatly enhanced by having a high-resolution structural model of the drug – protein complex. Towards this aim, a comprehensive study of an I –domain allosteric inhibitor complex to the I domain was undertaken, initially with the determination of the <sup>1</sup>H, <sup>15</sup>N and <sup>13</sup>C chemical shifts assignments of the full complex. The authors subsequently obtained multiple NOE distance based constraints between drug and protein, facilitating a high-resolution structure of the complex that could be used to rationalize the enhanced efficacy of the drug. As expected, the parent compound binds within the IDAS with a pocket formed by strands one, three and four of the central beta sheet and helices one and seven. Excellent superposition of the model with a crystal structure of the I domain – lovastatin complex validates the principle of using distinct molecular scaffolds to identify optimal allosteric inhibitors of I domain function.

## 6.2 SAR by NMR

Structure activity relationships by NMR (SAR by NMR) is an NMR based screening technology for discovering *de novo* or enhanced variants of existing protein inhibitors (Shuker et al., 1996). A library of small molecules is screened for binding to a protein target, typically by monitoring chemical shifts in a <sup>1</sup>H,<sup>15</sup>N HSQC experiment. Although most small fragments in the library bind to protein weakly, when joined synthetically the binding affinity and hopefully, efficacy of the composite molecule is improved dramatically. SAR by NMR may be used to identify completely novel combination of appropriate molecular fragments. Alternatively, the approach can be used to selectively enhance the affinity of one segment of a small molecule while leaving another fixed. In this context, the invariant moiety is added first to the NMR tube; subsequently, a library is screened to find appropriate binders with enhanced binding potential at the variable portion of the molecule. Finally, the novel molecular fragment is tethered synthetically to the fixed portion and the molecule is tested for the desired biological activity.

SAR by NMR was used to successfully improve the binding and efficacy of inhibitors based on an aryl cinnamide moiety (Liu et al., 2001; Winn et al., 2001). After identifying fragments that could potentially improve the inhibitor, the authors next obtained <sup>1</sup>H-<sup>1</sup>H NOEs of the ternary complex. The introduction of this additional step was a significant advance over simpler NMR screening protocols since it was possible to conclusively demonstrate that both fragments could bind to proximate but distinct regions on the protein. This extra step validated the potential of the separate fragments to mutually enhance protein binding when synthetically fused. These efforts led to the identification of a number of LFA-1 inhibitors with EC<sub>50</sub>s between 20 and 800 nM. In several cases the enhanced affinity was much less than anticipated based on the estimated binding affinity of the two fragments. However, this is not an unexpected phenomena since the linkers can both directly, through

interactions with the protein, and indirectly, by forcing unfavorable orientation/steric effects on the protein, lower the combined binding potential of the linked fragment with respect to that of the individual chemical moieties.

### 6.3 Peptides

Peptides, with sequences derived from the canonical binding protein ligand are an alternative source of integrin binding reagents. Generally, short peptides are unstructured in aqueous solution. Cyclization of the peptide through the backbone or appropriate side chain chemistries enhances the population of one or more structured states. Artificial non-genetically encoded amino acids are also introduced into the sequence as structural promoting agents or to add additional side chain chemistries.

Peptides, however, are particularly difficult to crystallize, particularly from aqueous solution. Also, crystal structures of small molecules and peptides are modulated by strong packing forces and the observed structure may be different from that in free solution or bound to a target protein. NMR spectroscopy can capture the full range of conformations sampled by the peptide and in appropriate systems, such as the I domain, also permits direct observation of both receptor free and receptor bound forms.

Two cyclic peptides, cIBR, derived from ICAM-1<sub>12-21</sub>, (Cyclo1,12-Pen-PRGGSVLVTGC-OH) and cIBC, derived from ICAM-1<sub>6-15</sub>, (Cyclo1,12-Pen-PSKVILPRGGC) have been shown to inhibit homotypic and heterotypic cell adhesion mediated by LFA-1 in a concentration dependent manner (Anderson et al., 2004). The peptides were cyclized through disulphide formation between the penicillamine moiety in position one and the cysteine at position twelve. Both peptides work, at least in part, via interactions with the I domain since their binding can be inhibited by the anti- $\alpha$ L-I domain antibody R3.1. Direct binding to intact soluble, TM free LFA-1 was demonstrated using a colorimetric ELISA binding assay. It is critical to note that although both peptides are derived from the authentic ligand, neither contains the canonical acidic group (in this case Glu34 of ICAM-1), suggesting an alternative mode of inhibition.

The structure of cIBR was determined by NMR spectroscopy in aqueous solution (Gursoy et al., 1999). The resonances were assigned using conventional through-bond (J-mediated) 2D-<sup>1</sup>H NMR spectra and inter-residue correlations from NOESY type experiments which were also used to obtain distance based constraints. Technically, the authors used a related pulse sequence called ROESY, a pulse sequence more suitable for obtaining distance constraints in low molecular weight systems. One experiment was performed to obtain the <sup>3</sup>J<sub>NH-HC $\alpha$</sub>  constants, another to determine the temperature dependence of the amide proton chemical shifts that are related to hydrogen bonding strength and thus indicative of presence of stable secondary structure. Molecular dynamics was used to obtain a set of structures for structural analysis. During the simulation, all the peptide bonds except the first (between Pen-1 and Pro-2) were held in the trans conformation. Final analysis of the structural ensemble revealed that a cis-conformer was present, albeit at low population and this form was not further studied.

Interactions between proximate amide protons observed in the ROESY spectrum suggest as many as 3  $\beta$ -turns about Pro2-Gly5, Gly5-Leu8, and Val9-Cys12 in the peptide structure, although it is unclear if all three turns are present in the structure simultaneously or are



inter-converting on a timescale slower than the NMR experiment. Additional data, namely the temperature dependence of amide protein chemical shift, suggests that the hydrogen bonds are weak and the structures are transiently populated.

In total, six structural families were obtained consistent with the NMR data, with each family containing 20 structures. Remarkably, some of the structures in the ensemble are in good agreement with the sequences in the context of the full-length domain 1 of ICAM-1. For example, the Pro-Arg-Gly-Gly sequence is derived from the  $\beta$ -hairpin turn connecting strands A and B of domain 1 of ICAM-1. Other regions of structural homology were also identified between peptide and full length protein, demonstrating that the small, cyclized peptide has captured at least some of the authentic architecture of the full-length ligand.

The binding site of both ICAM-1 derived peptides was measured using the perturbation in 2D-NMR heteronuclear chemical shifts approach previously described. As anticipated by the absence of an acidic group in the ligand, the NMR data suggest an alternative, allosteric mode of inhibition for the two peptides. Specifically, the binding site was identified as the IDAS, the binding pocket for small molecule antagonists (Zimmerman et al., 2007).

Although high resolution structural data was not obtained, the authors utilized the existing peptide structures, as well as the known structure of the I domain, to dock the peptides individually into the IDAS performing energy minimization to obtain a structural model which could reveal key interactions between peptide and protein. Intriguingly, despite being of entirely distinct classes of chemical moieties, it was possible to superimpose segments of the peptide on the known position of the lovastatin. The superposition revealed that common amino acids in the I domain contact the two distinct types of inhibitor. The model of the peptide – I domain revealed that, much like lovastatin, the hydrophobic residues of the peptide Gly 5- Gly 11 of cIBR are buried into the crevice with numerous hydrophobic contacts between the apolar core and the peptide. In general, the polar peptide regions of the peptide are exposed to solvent; however there is a putative salt bridge interaction between the arginine residue and Glu301 of the protein. Future high resolution studies will be required to provide important insight into the mechanism of recognition between peptide and I domain, the role of the flexible, hydrophilic peptide sequence in inhibiting integrin function, and to rationalize the superior performance of cIBR over cIBC as an LFA-1 antagonist. However, the cyclic ICAM-1 peptides were first designed using the rationale that competitive antagonists could be obtained using appropriately constrained elements of the native ligand sequence. These studies then demonstrate the power of basic, readily accessible NMR technology to test and refute mechanistic hypothesis of integrin antagonism.

#### 6.4 Volatile anesthetics

General anesthesia is administered to ~40 million patients undergoing surgery in the United States every year (Suttner et al., 2002). Volatile anesthetics (VAs), a group of lipophilic small molecules that induce general anesthesia, are a major component of the anesthetics drugs currently used in operating rooms worldwide. Nevertheless, our understanding of the mechanisms by which these small-molecules alter the activity of the CNS, thereby leading to the loss of consciousness, remains limited. The established molecular targets of VAs in the CNS include membrane-embedded ion channels; e.g.,  $\gamma$ -aminobutyric acid (GABA) type A receptors, two-pore-domain potassium channels, and N-methyl-D-aspartate (NMDA)



receptors. The aggregate of biochemical evidence suggests that VAs modulate ion channel functions in an allosteric, as opposed to a competitive, manner (Hemmings et al., 2005). The lack of high-resolution structural information regarding ion channels has made it impossible to determine the exact VA binding site(s) or mechanisms at work.

A unique feature of volatile anesthetic drugs is that the blood concentration at which these drugs exert pharmacological activities (i.e., induction of general anesthetic states) is high (0.1 to 1 mM). At these concentrations, anesthetics have been reported to affect not only neuronal cells but also diverse types of cells including leukocytes, platelets, endothelial cells, myocardial cells, bronchial epithelial cells, and cancer cells (McBride et al., 1996). Therefore, these secondary effects of VAs are of enormous clinical relevance and concern.

We investigated integrin interactions with volatile anesthetics for three reasons (Yuki et al., 2010; Yuki et al., 2008). First, we rationalized that the promiscuous nature of VA – protein interactions, in conjunction with the important role of LFA-1 function in the immune system made the protein a potential candidate for modulation by VA. Second, the I domain is a well-characterized, soluble protein amenable to biophysical and structural analysis. Beyond the direct physiological relevance of LFA-1 : VA interactions, we viewed the I domain as an ideal model system to understand how weakly binding VA could modulate protein function. Finally, the availability of NMR techniques would allow us to obtain a molecular mechanism for our observation that two volatile anesthetics, isoflurane and sevoflurane act as antagonists of LFA-1 binding to ICAM-1, both in cell and cell-free assays. NMR spectroscopy has been utilized in earlier studies of VA : protein interactions and demonstrated that it is possible to identify VA binding sites on proteins using NMR (Yonkunas et al., 2005). A critical difference between our studies and earlier investigations, is in the ability to perform activity assays on the I domain and directly compare anesthetic interactions with effect on biological functions. Previous studies have utilized model proteins that lack catalytic or adhesive activity and such comparisons were unavailable.

To map potential isoflurane binding site(s) in the LFA-1 I domain, we utilized heteronuclear  $^1\text{H},^{15}\text{N}$ -HSQC-NMR spectroscopy, an established technique for the identification of small-molecule interaction sites on isotopically labeled biomolecules, including anesthetic interactions with soluble protein domains (Yuki et al., 2008). An overlay of two HSQCs taken at the endpoints of an isoflurane titration (0 and 12 mM isoflurane, because high concentrations are preferred in order to fully occupy the binding site) not only revealed that a number of resonances undergo shifts in resonance frequency, but also identified the LFA-1 I domain as a potential binding site for isoflurane. The chemical shift of most residues was unchanged whether at the lowest (0 mM) or the highest (~12 mM) concentration of drug. However, several resonances, such as threonine 291 at top the loop that connects to the C-terminal helix, underwent a dose-dependent shift in resonance frequency, indicating an interaction and/or change in the electronic environment or local structure of the protein.

The magnitude of the isoflurane-induced shift was mapped onto the sequence and secondary structure (FIGURE 3). Significant chemical-shift perturbation occurred in six regions of the protein sequence: 1) the N-terminal segment; 2) the C-terminal portion of  $\beta 1$ ; 3) the loop between  $\beta 2$  and  $\beta 3$ ; 4)  $\beta 3$ ; 5)  $\beta 5$ ; and 6) the C-terminal segment incorporating  $\beta 5$ - $\alpha 7$ . Residues perturbed by the addition of the LFA-1 I allosteric antagonist lovastatin (visible as a uniform yellow background, **FIGURE 3**) showed a good correlation with those by isoflurane. The largest deviation in chemical shifts occurred with the aromatic resonances

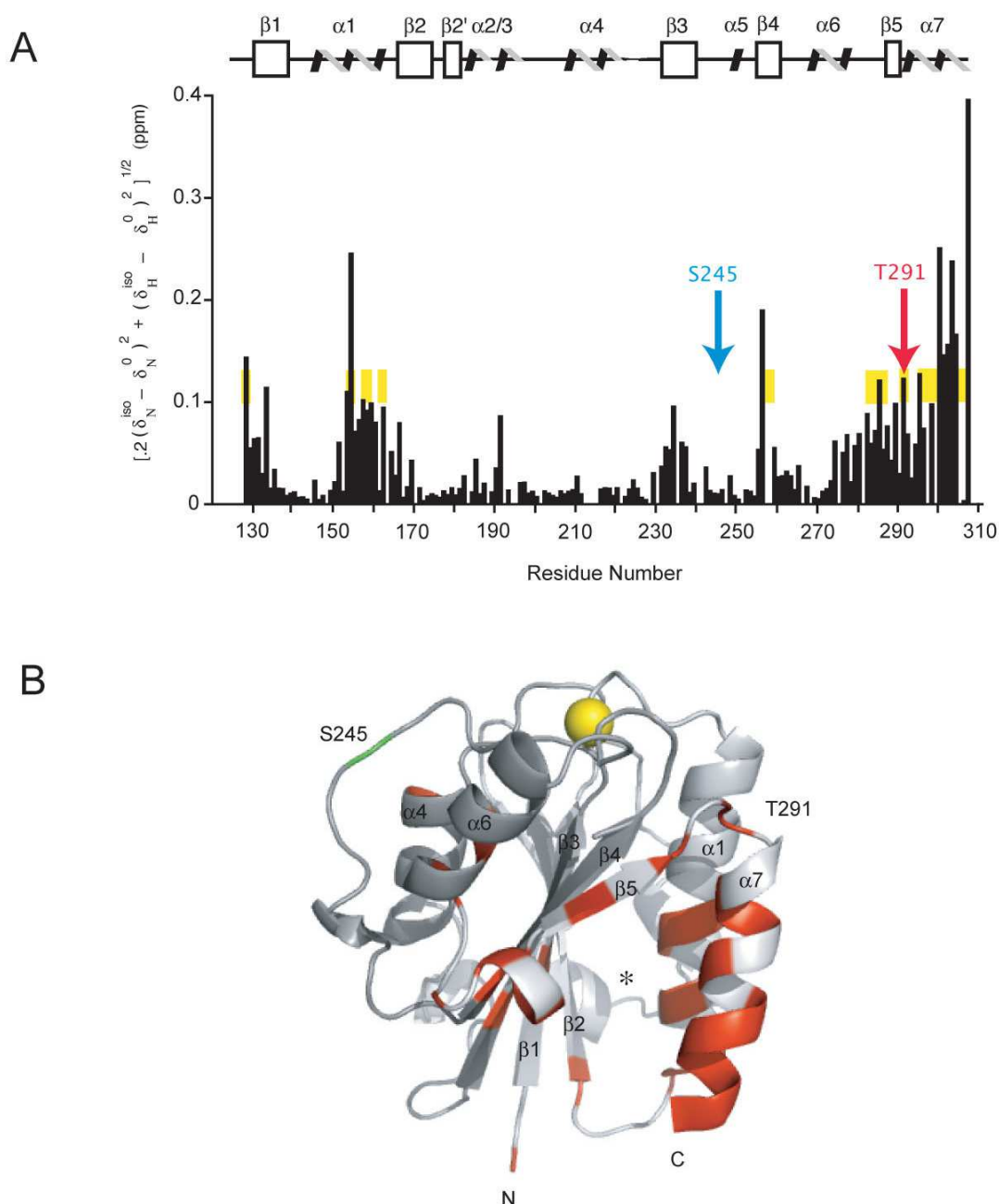


Fig. 3. NMR spectroscopy to study isoflurane-binding site(s) in the LFA-1 I (A) Scaled chemical-shift perturbation of 12 mM isoflurane mapped onto the LFA-1 I domain protein sequence and secondary structure. (B) Structure of the LFA-1 I domain showing amide nitrogen residues affected ( $\Delta\text{ppm} = 0.05$  ppm) by the addition of 12 mM isoflurane. Gray represents residues unperturbed by isoflurane while red represents residues that met or exceeded the threshold for perturbation. Helices and strands are labeled. Residues T291 (red) and S245 (green) are labeled. The yellow spheres represent the  $Mg^{2+}$  ion at the ICAM-1 binding site, termed the metal ion-dependent adhesion site (MIDAS). Note that the residues near the MIDAS were not affected and that the affected residues clustered near the cavity formed between the  $\alpha 1$  and  $\alpha 7$  helices and the central  $\beta$  strands. This figure was adopted from Yuki et al. 2008.

phenylalanine 153 (F153) and tyrosine 307 (Y307), which could indicate a direct interaction between the halogenated hydrocarbons and the aromatic moieties, as previously suggested. We note that Y307 is also an interacting residue in the derived model of cILB peptide with the I domain, suggesting a common mechanism of inhibition by the two remarkably different chemotypes. To generalize these results to other VA, we performed the same experiment using the VA sevoflurane (Yuki et al., 2010). Sevoflurane induced chemical shift perturbation in a subset of residues located at the C-terminal portion. This is consistent with the NMR data that we previously obtained from isoflurane's interaction with the LFA-1 I domain thereby suggesting that sevoflurane also binds to the C-terminal portion of the LFA-1 I domain, in which it blocks LFA-1 in the same allosteric manner that isoflurane does. By contrast, propofol, a distinct class of VA, induced perturbations to many residues spread over the I domain. The data is consistent with the idea that a high concentration of propofol inhibits LFA-1 in a mixed competitive and allosteric manner (NSA and MS, unpublished).

## 7. Saturation-Transfer Difference NMR (STD) and transferred NOE NMR studies

One of the central challenges faced in the study of integrin- antagonist interactions, particularly in the study of agonists which may interact with integrin domains that can-not be expressed in isolation such as the  $\beta$ - I like domain, is to determine the structure of the ligand bound complex. While docking and modeling studies, such as those described above, are valuable, changes in the conformation of the ligand and receptor can contribute to uncertainty in the molecular nature of complex formation. Saturation transfer difference NMR spectroscopy (STD-NMR), a technique originally developed to identify the carbohydrate epitope of protein lectins, has emerged as a powerful approach to overcome this difficulty (Mayer and Meyer, 1999). Because STD-NMR can be performed on proteins expressed in the native environment and does not require substantial quantities of protein, it is ideally suited to studying the interaction of cell surface transmembrane receptor interactions with potential antagonists. In fact, the high molecular weight of integrin in cell membranes – and even within cells – is advantageous since the saturation transfer effect improves with the molecular weight of the complex.

STD-NMR is based on the NMR effect of saturation. Prolonged irradiation of one or more spins by a long pulse or pulse train results in loss of signal intensity from the spectra of the irradiated spin. This saturation can propagate to neighboring spins through the dipolar interaction; the kinetics of the spread is favored in systems with high molecular weight. Because the transfer effect is through the dipolar coupling, the nuclei do not need to be covalently joined on the same molecule for saturation to spread between the spins. Thus saturation will result in the loss of signal intensity both for irradiated peaks and those spatially proximate. The saturation time can be manipulated to allow for propagation to proximate as opposed to distal spins, allowing for the mapping of direct binding epitopes between high-molecular weight protein systems and their ligands.

The STD-NMR experiment requires two sequential NMR spectra be obtained – one with and one without saturation. Because the experiment is performed with a large excess of ligand over protein, the saturation free spectrum is effectively identical to the spectrum of the free ligand. The high molecular weight of the membrane preparations or cells renders them undetectable by solution NMR. The second spectrum is acquired with saturation pulse(s)

applied selectively to a protein resonance. The saturation is then transferred to the ligand from the protein by the dipolar coupling. If the two spectra are subtracted, the difference spectrum only contains peaks from ligand resonances that were in contact with the protein during the saturation period. The STD effect is useful for characterizing protein-ligand complexes with weak-moderate binding constants ( $K_D \sim 1 \times 10^{-3}$  -  $K_D \sim 1 \times 10^{-8}$ ). This technique can be used to both validate the specificity of a binding interaction and map the epitope of nuclei that are directly bound to the protein since they undergo the greatest saturation effect.

STD-NMR was first applied to the study of cyclic-RGD peptides binding to purified  $\alpha IIb\beta 3$  integrin reconstituted into liposomes (Meinecke and Meyer, 2001). Using STD-NMR the authors determine an affinity  $K_D$  of 30-60  $\mu M$  for the peptide cyclo(RGDfv) complex with reconstituted integrin. No saturation effect was observed for liposomes free of integrin or non-ligand peptides with integrin containing liposomes, validating the specificity of the approach. Furthermore, a mixture of linear and cyclic RGD peptides gave rise only to spectra of the cyclic peptides, consistent with a previously established greater affinity for the cyclic versus linear peptide analogs. Analysis of the spectra and concentrations allowed for an estimate of  $\sim 1 mM$  for the  $K_D$  of the linear peptide. By comparison, the linear RGDS peptide, with a known  $K_D$  of 55  $\mu M$  was shown by STD-NMR to be an effective competitor of the cyclic-RGD peptide.

The authors further mapped the binding epitope of the peptide using the intensity of the resonances as a measure of proximity to the proteins surface. The largest signals were from the aromatic protons of the D-Phe followed by the Arg  $H\alpha$ , Arg  $H\beta/H\gamma$ , Asp  $H\beta$  and the  $\beta$ -protons of the unnatural amino acid D-Hph residue as well as the  $\gamma$ -protons of Val, the  $H\alpha$  proton of Gly, demonstrating that these were the atoms directly contact with integrin. Prior studies on the conformation of the RGDfv cyclic peptide in DMSO by 2D-NMR structural methods was used to interpret the epitope mapping investigation (Aumailley et al., 1991). In the NMR structure, the side chains of Arg, Asp and Val are disposed perpendicular to the plane of the peptide and point to one side. The D-Phe side chain is located in an equatorial conformation. These suggest that the ligand interactions on one side of the peptide ring with the Phe in the equatorial position making further stabilizing interactions. The pattern of the Arg alkyl side chain suggests that strongly hydrophobic interactions are predominant while the Arg  $\delta$ -protons, which would be indicative of the tight interaction of the guanidine group, are only weakly saturated. Although this is at first surprising, given the conservation of the Arg in the canonical binding motif, the L-amino acids norleucine, cyclohexylglycine, norvaline, tert-leucine and 4-hydroxyproline all have tighter affinity in the position occupied by Arg than the Arg itself, suggesting that the ionic interaction makes little or no contribution to the stability of the complex. Also, the high intensity of the D-Phe resonance is consistent with the fact that hydrophobic and aromatic residues that are adjacent to the Asp have greater inhibitory potential, both in natural disintegrin proteins and designed inhibitor peptides. This effect is exploited in  $\alpha IIb\beta 3$  specific platelet inhibitors including the cyclic hepta-peptide eptifibatide, which has a L-homoarginine in the first position (Scarborough et al., 1993). Thus the extended alkyl chain in the first position and the aromatic in the fourth position of this optimized  $\alpha IIb\beta 3$  inhibitor are both consistent with the results of the STD-NMR studies of the binding epitope.



A comparison between STD-experiments obtained on liposomal preparations with  $\alpha\text{IIb}\beta 3$  on the surface of platelets was obtained with interesting results (Claasen et al., 2005). Although the binding epitope in the two experimental contexts is almost identical (with minor variations) the STD effect was much higher in the intact platelet preparation, despite the fact that the concentration of receptor in the liposomal sample is  $\sim 5 \mu\text{M}$  and only  $\sim 0.6 \mu\text{M}$  for the platelet sample, demonstrating the affinity, of  $\alpha\text{IIb}\beta 3$  for the ligand is significantly higher in the native context. This demonstrates the great utility of STD-NMR that can determine both epitopes and approximate measure of antagonist affinity on intact cells. Assuming 150,000 receptors/cell,  $10^8$  or fewer cells are required to obtain an STD-NMR spectrum with good signal to noise, a number that can readily be accommodated in a standard NMR tube.

A powerful feature of the STD-NMR experiment is consequently the ability to obtain binding information directly on the cells targeted by a therapeutic agent of interest (Potenza et al., 2011). One such study examined the binding of two closely related cyclic-RGD peptides with dramatically different  $\text{IC}_{50}$ s to the integrin  $\alpha\text{V}\beta 3$  on EVC304, a bladder cancer cell line. The two cyclic peptides, with competitive  $\text{IC}_{50}$ s of 6.4 nM versus 154 nM against echistatin binding differ in the configuration about two stereo-centers and are known, from earlier NMR studies of the free inhibitor, to have distinct conformations in the unbound state. The STD-NMR derived epitope of the stronger binding cyclic-peptide that has a  $\mu\text{M}$   $\text{IC}_{50}$  for inhibiting cell adhesion to ECM ligands agrees with a previously derived docking model. The ligand interacts through a pair of ionic interactions (Arg-guandinium with  $\alpha\text{V}\text{-Asp}218$  and Asp-carboxyl with the  $\beta 3\text{-MIDAS}$ ), a  $\pi\text{-}\pi$  interaction (between a benzylic group on the ligand and an aromatic ring of  $\beta 3\text{-Tyr}122$ ) and an extended network of hydrogen bonds including the Asp-NH and C=O of  $\beta 3\text{-Arg}216$ . The overall structure of the cyclic peptide closely resembles the high-resolution crystal structure of the peptide cingetide bound to  $\alpha\text{V}\beta 3$ .

The authors used a second technique, transferred NOE (TR-NOE) spectroscopy, to obtain the conformation of the bound ligand. TR-NOE is an NMR experiment that permits the selective observation of ligand NOEs through space correlations present in the low population bound form of a complex to be observed in the high population free state. Using this technique, it was possible to identify conformational changes in the ligand that are required for ligand binding.

STD-NMR of the weaker binding cyclic peptide was also obtained using STD-NMR and revealed a distinct binding epitope. The most significant change, due to the altered conformation around the two stereocenters, was the loss of the hydrogen bonding network between ligand Asp and the  $\beta$ -subunit. The authors also using TR-NOE observed conformational changes between the ligand in the free and bound state. The bound conformation of the second inhibitor forms less favorable contacts with the integrin, accounting for the loss of inhibition efficacy.

One important extension of the STD-NMR experiments is the incorporation of heteronuclear 2D detection, which is required to determine the epitope of more complex peptides and proteins that would otherwise be difficult to study due to resonance overlap (Assadi-Porter et al., 2010; Wagstaff et al., 2010b). A recent investigation both demonstrated both the overall utility of STD-NMR for study of integrin-antagonist interactions and also the advantages of using 2D NMR to as opposed to 1D detection despite the added time and expense of



preparing the requisite isotopic labeled sample(s). The authors studied a complex of  $\alpha V\beta 6$  with a peptide inhibitor derived from the surface loop of the foot and mouth virus capsid protein, which utilizes this integrin as a receptor. The peptide, A20FMDV2, has the sequence NAVPNLRGDLQVLAQKVART. Previous work showed that peptide inhibitors of  $\alpha V\beta 6$  utilize the extended sequence DLXXLRGD as an extended recognition motif. To obtain the isotopic labeled peptide, the authors utilized a commercial *E. coli* fusion peptide system whereby the peptide is fused to the insoluble ketosteroid isomerase protein with a methionine residue introduced between KSI and the peptide sequence. The insoluble fusion pair is readily separated from the soluble cell material and then can be cleaved using cyanogen bromide treatment (Wagstaff et al., 2010a).

The 2D- $^{13}\text{C}$  STD-NMR experiments demonstrate a pronounced contribution from the DLXXL motif to the binding epitope and, surprising, a less substantial component from the RGD regions. Significantly, an earlier 1D-STD-NMR misidentified part of the binding epitope, due to uncertainty in the resonance assignments that occur due to overlap in the NMR spectrum. The primary interaction between peptide and protein is through  $^6\text{Leu}$ ,  $^{12}\text{Val}$  and  $^{13}\text{Leu}$ . Despite not obtaining any high resolution (i.e. NOE or J-coupling) constraints, the authors were able to utilize intensity and phase information (both sensitive to the saturation transfer efficiency) of resonances from the  $^1\text{H}$ - $^{13}\text{C}$  and  $^1\text{H}$ - $^{15}\text{N}$  detected STD-NMR experiments to construct a refined model of the peptide-integrin interaction which is of great utility in the design of novel peptide and peptide-mimetic inhibitors.

## 8. Conclusions

To build upon the advances described in this review, we have identified five critical areas which we feel will contribute to a greater understanding of the mechanism of integrin activation and the development of improved antagonists targeting integrin function.

*Automation:* Conventional NMR spectroscopy requires the determination of resonance assignments to extract meaningful spectroscopic data. The process of resonance assignment is, however, manually intensive and cumbersome, especially given the need to screen large number of potential binding reagents to a molecular target. There has, however, been recent progress in automating the assignment and structure determination and analysis process (Guerry and Herrmann, 2011). In particular, methods which permit partial assignments of putative ligand binding interfaces without resorting to total assignment or structure determination would greatly facilitate the utility of NMR as a high-throughput screening tool. One recent advance in this area applied to the development of integrin antagonists is the technique of Methyl Scanning. Because many I domain inhibitors contain aromatic rings that can induce large chemical shifts in proximal aliphatic side chain resonances, partial assignments of methyl carbons and protons can serve as a useful source of constraints probing ligand binding to suitable protein pockets. This technique was recently employed to study the mechanism of a tight binding (18.3 nM) arylthio allosteric inhibitor of the LFA-1 I domain (Constantine et al., 2006).

*Expression and Labeling:* Although the I domain can be produced in isolation of other integrin domains using standard *E. coli* expression systems, other critical integrin domains require domain-domain interactions for correct folding. This precludes the use of basic *E. coli* expression systems that are optimal for preparing the isotope labeled samples used in high

resolution NMR studies. Recent advances in two areas promise to break through this bottleneck. First, the use of eukaryotic expression either in yeast or mammalian cells has been demonstrated to produce quantities of protein suitable for NMR studies. *In vitro* translation systems have also been optimized to produce suitable quantities of isotopic labeled proteins and represent a viable alternative approach to producing complex multidomain proteins of eukaryotic origin (Yokoyama, 2003).

*Transmembrane and cytoplasmic domains:* Separation of the transmembrane and cytoplasmic domains is a critical step in integrin activation. While existing integrin modulators work by stabilizing the inactive conformation of the ecto- domains, there has been recent interest in pharmacological targeting of transmembrane structure (Shandler et al., 2011). However, transmembrane domains pose a particular challenge for conventional solution NMR due to the large molecular weight of the bilayer required to maintain the protein in the correct conformation. Recent advances in solution NMR, particularly the development of membrane nanodiscs that preserve the authentic structure of the native bilayer, have begun to overcome this limitation and provide detailed, high-resolution structural details on association of transmembrane peptides (Warschawski et al., 2011).

*Dynamics:* While the role of protein dynamics in protein function, and inhibition have been widely appreciated, there has been renewed development in methods that can be obtained with site-specific resolution. A major existing challenge is the incorporation of dynamics information into docking and screening protocols. In this area, improved computational protocols will be needed to parallel the increased ability to observe and quantify chemical exchange processes in proteins. New methods for incorporation of dynamics data into drug discovery protocols will likely be of comparable importance to the introduction of structural constraints (Lin, 2011; Salsbury, 2010).

*Crystal Structures:* Paradoxically, the most urgent need in the area of NMR based integrin drug design is for additional crystal structures both of new integrins as well as drug – integrin complexes. While NMR is a powerful structural tool in its own right, the true power of NMR lies in the capacity to rapidly determine structural and dynamic information of ligands and their binding sites that can be integrated with existing structures using computational modeling tools. The most successful future structure based design approaches are likely to integrate multiple sources of information to identify the most optimal drug candidates for biological screening.

## 9. References

- Alonso, J.L., Essafi, M., Xiong, J.P., Stehle, T., and Arnaout, M.A. (2002). Does the integrin alphaA domain act as a ligand for its betaA domain? *Curr Biol* 12, R340-342.
- Anderson, M.E., Yakovleva, T., Hu, Y., and Siahhaan, T.J. (2004). Inhibition of ICAM-1/LFA-1-mediated heterotypic T-cell adhesion to epithelial cells: design of ICAM-1 cyclic peptides. *Bioorg Med Chem Lett* 14, 1399-1402.
- Assadi-Porter, F.M., Tonelli, M., Maillet, E.L., Markley, J.L., and Max, M. (2010). Interactions between the human sweet-sensing T1R2-T1R3 receptor and sweeteners detected by saturation transfer difference NMR spectroscopy. *Biochim Biophys Acta* 1798, 82-86.

- Aumailley, M., Gurrath, M., Muller, G., Calvete, J., Timpl, R., and Kessler, H. (1991). Arg-Gly-Asp constrained within cyclic pentapeptides. Strong and selective inhibitors of cell adhesion to vitronectin and laminin fragment P1. *FEBS Lett* 291, 50-54.
- Beglova, N., Blacklow, S.C., Takagi, J., and Springer, T.A. (2002). Cysteine-rich module structure reveals a fulcrum for integrin rearrangement upon activation. *Nat Struct Biol* 9, 282-287.
- Bhunia, A., Tang, X.Y., Mohanram, H., Tan, S.M., and Bhattacharjya, S. (2009). NMR solution conformations and interactions of integrin  $\alpha$ L $\beta$ 2 cytoplasmic tails. *J Biol Chem* 284, 3873-3884.
- Campbell, I.D., and Humphries, M.J. (2011). Integrin structure, activation, and interactions. *Cold Spring Harb Perspect Biol* 3.
- Cavanagh, J., Fairbrother, W., AG Palmer III, and Skelton, N. (2006). *Protein NMR Spectroscopy, Second Edition: Principles and Practice* (San Diego, CA, Academic Press).
- Cicala, C., Arthos, J., and Fauci, A.S. (2011). HIV-1 envelope, integrins and co-receptor use in mucosal transmission of HIV. *J Transl Med* 9 Suppl 1, S2.
- Claasen, B., Axmann, M., Meinecke, R., and Meyer, B. (2005). Direct observation of ligand binding to membrane proteins in living cells by a saturation transfer double difference (STDD) NMR spectroscopy method shows a significantly higher affinity of integrin  $\alpha$ (IIb) $\beta$ 3 in native platelets than in liposomes. *J Am Chem Soc* 127, 916-919.
- Coller, B.S., and Shattil, S.J. (2008). The GPIIb/IIIa (integrin  $\alpha$ IIb $\beta$ 3) odyssey: a technology-driven saga of a receptor with twists, turns, and even a bend. *Blood* 112, 3011-3025.
- Constantine, K.L., Davis, M.E., Metzler, W.J., Mueller, L., and Claus, B.L. (2006). Protein-ligand NOE matching: a high-throughput method for binding pose evaluation that does not require protein NMR resonance assignments. *J Am Chem Soc* 128, 7252-7263.
- Crump, M.P., Ceska, T.A., Spyropoulos, L., Henry, A., Archibald, S.C., Alexander, R., Taylor, R.J., Findlow, S.C., O'Connell, J., Robinson, M.K., et al. (2004). Structure of an allosteric inhibitor of LFA-1 bound to the I-domain studied by crystallography, NMR, and calorimetry. *Biochemistry* 43, 2394-2404.
- Cuzange, A., Chroboczek, J., and Jacrot, B. (1994). The penton base of human adenovirus type 3 has the RGD motif. *Gene* 146, 257-259.
- Dijkgraaf, I., Beer, A.J., and Wester, H.J. (2009). Application of RGD-containing peptides as imaging probes for  $\alpha$ v $\beta$ 3 expression. *Front Biosci* 14, 887-899.
- Ding, Z.M., Babensee, J.E., Simon, S.I., Lu, H., Perrard, J.L., Bullard, D.C., Dai, X.Y., Bromley, S.K., Dustin, M.L., Entman, M.L., et al. (1999). Relative contribution of LFA-1 and Mac-1 to neutrophil adhesion and migration. *J Immunol* 163, 5029-5038.
- Ege, S. (2003). *Organic Chemistry: Structure and Reactivity* (Chicago, IL, Houghton Mifflin Harcourt).
- Evans, R., Patzak, I., Svensson, L., De Filippo, K., Jones, K., McDowall, A., and Hogg, N. (2009). Integrins in immunity. *J Cell Sci* 122, 215-225.
- Fagerholm, S.C., Hilden, T.J., and Gahmberg, C.G. (2004). P marks the spot: site-specific integrin phosphorylation regulates molecular interactions. *Trends Biochem Sci* 29, 504-512.

- Fleming, F.E., Graham, K.L., Taniguchi, K., Takada, Y., and Coulson, B.S. (2007). Rotavirus-neutralizing antibodies inhibit virus binding to integrins alpha 2 beta 1 and alpha 4 beta 1. *Arch Virol* 152, 1087-1101.
- Gaillard, T., Martin, E., San Sebastian, E., Cossio, F.P., Lopez, X., Dejaegere, A., and Stote, R.H. (2007). Comparative normal mode analysis of LFA-1 integrin I-domains. *J Mol Biol* 374, 231-249.
- George, E.L., Georges-Labouesse, E.N., Patel-King, R.S., Rayburn, H., and Hynes, R.O. (1993). Defects in mesoderm, neural tube and vascular development in mouse embryos lacking fibronectin. *Development* 119, 1079-1091.
- Gottschalk, K.E. (2005). A coiled-coil structure of the alphaIIb beta3 integrin transmembrane and cytoplasmic domains in its resting state. *Structure* 13, 703-712.
- Guerry, P., and Herrmann, T. (2011). Advances in automated NMR protein structure determination. *Q Rev Biophys* 44, 257-309.
- Gursoy, R.N., Jois, D.S., and Siahhaan, T.J. (1999). Structural recognition of an ICAM-1 peptide by its receptor on the surface of T cells: conformational studies of cyclo (1, 12)-Pen-Pro-Arg-Gly-Gly-Ser-Val-Leu-Val-Thr-Gly-Cys-OH. *J Pept Res* 53, 422-431.
- Hemmings, H.C., Jr., Akabas, M.H., Goldstein, P.A., Trudell, J.R., Orser, B.A., and Harrison, N.L. (2005). Emerging molecular mechanisms of general anesthetic action. *Trends Pharmacol Sci* 26, 503-510.
- Huth, J.R., Olejniczak, E.T., Mendoza, R., Liang, H., Harris, E.A., Lupher, M.L., Jr., Wilson, A.E., Fesik, S.W., and Staunton, D.E. (2000). NMR and mutagenesis evidence for an I domain allosteric site that regulates lymphocyte function-associated antigen 1 ligand binding. *Proc Natl Acad Sci U S A* 97, 5231-5236.
- Hynes, R.O. (2002). Integrins: bidirectional, allosteric signaling machines. *Cell* 110, 673-687.
- Imai, Y., Park, E.J., Peer, D., Peixoto, A., Cheng, G., von Andrian, U.H., Carman, C.V., and Shimaoka, M. (2008). Genetic perturbation of the putative cytoplasmic membrane-proximal salt bridge aberrantly activates alpha(4) integrins. *Blood* 112, 5007-5015.
- Jin, H., and Varner, J. (2004). Integrins: roles in cancer development and as treatment targets. *Br J Cancer* 90, 561-565.
- Jin, M., Andricioaei, I., and Springer, T.A. (2004). Conversion between three conformational states of integrin I domains with a C-terminal pull spring studied with molecular dynamics. *Structure* 12, 2137-2147.
- Kallen, J., Welzenbach, K., Ramage, P., Geyl, D., Kriwacki, R., Legge, G., Cottens, S., Weitz-Schmidt, G., and Hommel, U. (1999). Structural basis for LFA-1 inhibition upon lovastatin binding to the CD11a I-domain. *J Mol Biol* 292, 1-9.
- Kriwacki, R.W., Legge, G.B., Hommel, U., Ramage, P., Chung, J., Tennant, L.L., Wright, P.E., and Dyson, H.J. (2000). Assignment of <sup>1</sup>H, <sup>13</sup>C and <sup>15</sup>N resonances of the I-domain of human leukocyte function associated antigen-1. *J Biomol NMR* 16, 271-272.
- Lambert, L.J., Bobkov, A.A., Smith, J.W., and Marassi, F.M. (2008). Competitive interactions of collagen and a jararhagin-derived disintegrin peptide with the integrin alpha2-I domain. *J Biol Chem* 283, 16665-16672.
- Lee, J.O., Bankston, L.A., Arnaout, M.A., and Liddington, R.C. (1995a). Two conformations of the integrin A-domain (I-domain): a pathway for activation? *Structure* 3, 1333-1340.
- Lee, J.O., Rieu, P., Arnaout, M.A., and Liddington, R. (1995b). Crystal structure of the A domain from the alpha subunit of integrin CR3 (CD11b/CD18). *Cell* 80, 631-638.



- Legge, G.B., Kriwacki, R.W., Chung, J., Hommel, U., Ramage, P., Case, D.A., Dyson, H.J., and Wright, P.E. (2000). NMR solution structure of the inserted domain of human leukocyte function associated antigen-1. *J Mol Biol* 295, 1251-1264.
- Li, R., Babu, C.R., Valentine, K., Lear, J.D., Wand, A.J., Bennett, J.S., and DeGrado, W.F. (2002). Characterization of the monomeric form of the transmembrane and cytoplasmic domains of the integrin beta 3 subunit by NMR spectroscopy. *Biochemistry* 41, 15618-15624.
- Lin, J.H. (2011). Accommodating protein flexibility for structure-based drug design. *Curr Top Med Chem* 11, 171-178.
- Liu, G., Huth, J.R., Olejniczak, E.T., Mendoza, R., DeVries, P., Leitza, S., Reilly, E.B., Okasinski, G.F., Fesik, S.W., and von Geldern, T.W. (2001). Novel p-arylthio cinnamides as antagonists of leukocyte function-associated antigen-1/intracellular adhesion molecule-1 interaction. 2. Mechanism of inhibition and structure-based improvement of pharmaceutical properties. *J Med Chem* 44, 1202-1210.
- Lu, C., Shimaoka, M., Ferzly, M., Oxvig, C., Takagi, J., and Springer, T.A. (2001a). An isolated, surface-expressed I domain of the integrin alphaLbeta2 is sufficient for strong adhesive function when locked in the open conformation with a disulfide bond. *Proc Natl Acad Sci U S A* 98, 2387-2392.
- Lu, C., Shimaoka, M., Zang, Q., Takagi, J., and Springer, T.A. (2001b). Locking in alternate conformations of the integrin alphaLbeta2 I domain with disulfide bonds reveals functional relationships among integrin domains. *Proc Natl Acad Sci U S A* 98, 2393-2398.
- Lu, C., Takagi, J., and Springer, T.A. (2001c). Association of the membrane proximal regions of the alpha and beta subunit cytoplasmic domains constrains an integrin in the inactive state. *J Biol Chem* 276, 14642-14648.
- Luo, B.H., Carman, C.V., and Springer, T.A. (2007). Structural basis of integrin regulation and signaling. *Annu Rev Immunol* 25, 619-647.
- Luo, B.H., Springer, T.A., and Takagi, J. (2004). A specific interface between integrin transmembrane helices and affinity for ligand. *PLoS Biol* 2, e153.
- Mayer, M., and Meyer, B. (1999). Characterization of ligand binding by saturation transfer difference NMR spectroscopy. *Angewandte Chemie* 38, 1784-1788.
- McBride, W.T., Armstrong, M.A., and McBride, S.J. (1996). Immunomodulation: an important concept in modern anaesthesia. *Anaesthesia* 51, 465-473.
- Meinecke, R., and Meyer, B. (2001). Determination of the binding specificity of an integral membrane protein by saturation transfer difference NMR: RGD peptide ligands binding to integrin alphaIIb beta3. *J Med Chem* 44, 3059-3065.
- Mittermaier, A., and Kay, L.E. (2006). New tools provide new insights in NMR studies of protein dynamics. *Science* 312, 224-228.
- Nemeth, J.A., Nakada, M.T., Trikha, M., Lang, Z., Gordon, M.S., Jayson, G.C., Corringham, R., Prabhakar, U., Davis, H.M., and Beckman, R.A. (2007). Alpha-v integrins as therapeutic targets in oncology. *Cancer Invest* 25, 632-646.
- Nishida, N., Xie, C., Shimaoka, M., Cheng, Y., Walz, T., and Springer, T.A. (2006). Activation of leukocyte beta2 integrins by conversion from bent to extended conformations. *Immunity* 25, 583-594.

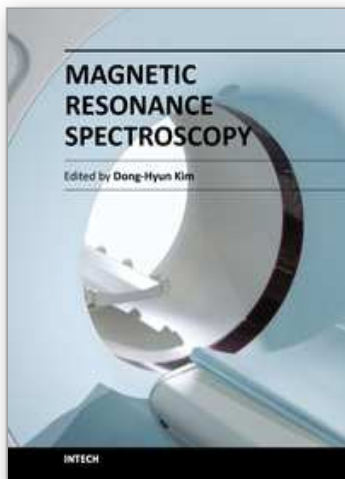


- Palmer, A.G., 3rd, and Massi, F. (2006). Characterization of the dynamics of biomacromolecules using rotating-frame spin relaxation NMR spectroscopy. *Chem Rev* 106, 1700-1719.
- Park, E.J., Mora, J.R., Carman, C.V., Chen, J., Sasaki, Y., Cheng, G., von Andrian, U.H., and Shimaoka, M. (2007). Aberrant activation of integrin  $\alpha 4 \beta 7$  suppresses lymphocyte migration to the gut. *J Clin Invest* 117, 2526-2538.
- Plow, E.F., Haas, T.A., Zhang, L., Loftus, J., and Smith, J.W. (2000). Ligand binding to integrins. *J Biol Chem* 275, 21785-21788.
- Potenza, D., Vasile, F., Belvisi, L., Civera, M., and Araldi, E.M. (2011). STD and trNOESY NMR study of receptor-ligand interactions in living cancer cells. *Chembiochem* 12, 695-699.
- Qu, A., and Leahy, D.J. (1995). Crystal structure of the I-domain from the CD11a/CD18 (LFA-1,  $\alpha L \beta 2$ ) integrin. *Proc Natl Acad Sci U S A* 92, 10277-10281.
- Reardon, D.A., Fink, K.L., Mikkelsen, T., Cloughesy, T.F., O'Neill, A., Plotkin, S., Glantz, M., Ravin, P., Raizer, J.J., Rich, K.M., et al. (2008). Randomized phase II study of cilengitide, an integrin-targeting arginine-glycine-aspartic acid peptide, in recurrent glioblastoma multiforme. *J Clin Oncol* 26, 5610-5617.
- Ruoslahti, E. (1996). RGD and other recognition sequences for integrins. *Annu Rev Cell Dev Biol* 12, 697-715.
- Salsbury, F.R., Jr. (2010). Molecular dynamics simulations of protein dynamics and their relevance to drug discovery. *Curr Opin Pharmacol* 10, 738-744.
- Scarborough, R.M. (1999). Development of eptifibatide. *Am Heart J* 138, 1093-1104.
- Scarborough, R.M., Naughton, M.A., Teng, W., Rose, J.W., Phillips, D.R., Nannizzi, L., Arfsten, A., Campbell, A.M., and Charo, I.F. (1993). Design of potent and specific integrin antagonists. Peptide antagonists with high specificity for glycoprotein IIb-IIIa. *J Biol Chem* 268, 1066-1073.
- Schorberg, K.L., Shoemaker, C.J., Dube, D., Abshire, M.Y., Delos, S.E., Bouton, A.H., and White, J.M. (2009).  $\alpha 5 \beta 1$ -integrin controls ebolavirus entry by regulating endosomal cathepsins. *Proc Natl Acad Sci U S A* 106, 8003-8008.
- Semrich, M., Smith, A., Feterowski, C., Beer, S., Engelhardt, B., Busch, D.H., Bartsch, B., Laschinger, M., Hogg, N., Pfeffer, K., et al. (2005). Importance of integrin LFA-1 deactivation for the generation of immune responses. *J Exp Med* 201, 1987-1998.
- Shamri, R., Grabovsky, V., Gauguier, J.M., Feigelson, S., Manevich, E., Kolanus, W., Robinson, M.K., Staunton, D.E., von Andrian, U.H., and Alon, R. (2005). Lymphocyte arrest requires instantaneous induction of an extended LFA-1 conformation mediated by endothelium-bound chemokines. *Nat Immunol* 6, 497-506.
- Shandler, S.J., Korendovych, I.V., Moore, D.T., Smith-Dupont, K.B., Streu, C.N., Litvinov, R.I., Billings, P.C., Gai, F., Bennett, J.S., and Degrad, W.F. (2011). Computational Design of a  $\beta$ -Peptide That Targets Transmembrane Helices. *J Am Chem Soc* 133, 12378-12381.
- Shimaoka, M., and Springer, T.A. (2003). Therapeutic antagonists and conformational regulation of integrin function. *Nat Rev Drug Discov* 2, 703-716.
- Shimaoka, M., Takagi, J., and Springer, T.A. (2002). Conformational regulation of integrin structure and function. *Annu Rev Biophys Biomol Struct* 31, 485-516.

- Shimaoka, M., Xiao, T., Liu, J.H., Yang, Y., Dong, Y., Jun, C.D., McCormack, A., Zhang, R., Joachimiak, A., Takagi, J., et al. (2003). Structures of the alpha L I domain and its complex with ICAM-1 reveal a shape-shifting pathway for integrin regulation. *Cell* 112, 99-111.
- Shuker, S.B., Hajduk, P.J., Meadows, R.P., and Fesik, S.W. (1996). Discovering high-affinity ligands for proteins: SAR by NMR. *Science* 274, 1531-1534.
- Suttner, S., Kumle, B., and Boldt, J. (2002). Pharmacoeconomic considerations in anaesthetic use. *Expert Opin Pharmacother* 3, 1267-1272.
- Takagi, J., Beglova, N., Yalamanchili, P., Blacklow, S.C., and Springer, T.A. (2001). Definition of EGF-like, closely interacting modules that bear activation epitopes in integrin beta subunits. *Proc Natl Acad Sci U S A* 98, 11175-11180.
- Vinogradova, O., Velyvis, A., Velyviene, A., Hu, B., Haas, T., Plow, E., and Qin, J. (2002). A structural mechanism of integrin alpha(IIb)beta(3) "inside-out" activation as regulated by its cytoplasmic face. *Cell* 110, 587-597.
- Wagstaff, J.L., Howard, M.J., and Williamson, R.A. (2010a). Production of recombinant isotopically labelled peptide by fusion to an insoluble partner protein: generation of integrin alphavbeta6 binding peptides for NMR. *Mol Biosyst* 6, 2380-2385.
- Wagstaff, J.L., Vallath, S., Marshall, J.F., Williamson, R.A., and Howard, M.J. (2010b). Two-dimensional heteronuclear saturation transfer difference NMR reveals detailed integrin alphavbeta6 protein-peptide interactions. *Chem Commun (Camb)* 46, 7533-7535.
- Warschawski, D.E., Arnold, A.A., Beaugrand, M., Gravel, A., Chartrand, E., and Marcotte, I. (2011). Choosing membrane mimetics for NMR structural studies of transmembrane proteins. *Biochim Biophys Acta* 1808, 1957-1974.
- Weitz-Schmidt, G., Welzenbach, K., Brinkmann, V., Kamata, T., Kallen, J., Bruns, C., Cottens, S., Takada, Y., and Hommel, U. (2001). Statins selectively inhibit leukocyte function antigen-1 by binding to a novel regulatory integrin site. *Nat Med* 7, 687-692.
- Winn, M., Reilly, E.B., Liu, G., Huth, J.R., Jae, H.S., Freeman, J., Pei, Z., Xin, Z., Lynch, J., Kester, J., et al. (2001). Discovery of novel p-arylthio cinnamides as antagonists of leukocyte function-associated antigen-1/intercellular adhesion molecule-1 interaction. 4. Structure-activity relationship of substituents on the benzene ring of the cinnamide. *J Med Chem* 44, 4393-4403.
- Wouters, M.A., Rigoutsos, I., Chu, C.K., Feng, L.L., Sparrow, D.B., and Dunwoodie, S.L. (2005). Evolution of distinct EGF domains with specific functions. *Protein Sci* 14, 1091-1103.
- Wuthrich, K. (1986). *NMR of Proteins and Nucleic Acids* (New York, John Wiley and Sons).
- Xiao, T., Takagi, J., Collier, B.S., Wang, J.H., and Springer, T.A. (2004). Structural basis for allostery in integrins and binding to fibrinogen-mimetic therapeutics. *Nature* 432, 59-67.
- Xie, C., Shimaoka, M., Xiao, T., Schwab, P., Klickstein, L.B., and Springer, T.A. (2004). The integrin alpha-subunit leg extends at a Ca<sup>2+</sup>-dependent epitope in the thigh/genu interface upon activation. *Proc Natl Acad Sci U S A* 101, 15422-15427.
- Xiong, J.P., Goodman, S.L., and Arnaout, M.A. (2007). Purification, analysis, and crystal structure of integrins. *Methods in enzymology* 426, 307-336.

- Xiong, J.P., Li, R., Essafi, M., Stehle, T., and Arnaout, M.A. (2000). An isoleucine-based allosteric switch controls affinity and shape shifting in integrin CD11b A-domain. *J Biol Chem* 275, 38762-38767.
- Xiong, J.P., Stehle, T., Diefenbach, B., Zhang, R., Dunker, R., Scott, D.L., Joachimiak, A., Goodman, S.L., and Arnaout, M.A. (2001). Crystal structure of the extracellular segment of integrin alpha Vbeta3. *Science* 294, 339-345.
- Xiong, J.P., Stehle, T., Zhang, R., Joachimiak, A., Frech, M., Goodman, S.L., and Arnaout, M.A. (2002). Crystal structure of the extracellular segment of integrin alpha Vbeta3 in complex with an Arg-Gly-Asp ligand. *Science* 296, 151-155.
- Yang, J.T., Rayburn, H., and Hynes, R.O. (1993). Embryonic mesodermal defects in alpha 5 integrin-deficient mice. *Development* 119, 1093-1105.
- Yokoyama, S. (2003). Protein expression systems for structural genomics and proteomics. *Curr Opin Chem Biol* 7, 39-43.
- Yonkunas, M.J., Xu, Y., and Tang, P. (2005). Anesthetic interaction with ketosteroid isomerase: insights from molecular dynamics simulations. *Biophys J* 89, 2350-2356.
- Yoon, C.S., Kim, K.D., Park, S.N., and Cheong, S.W. (2001). alpha(6) Integrin is the main receptor of human papillomavirus type 16 VLP. *Biochem Biophys Res Commun* 283, 668-673.
- Yuki, K., Astrof, N.S., Bracken, C., Soriano, S.G., and Shimaoka, M. (2010). Sevoflurane binds and allosterically blocks integrin lymphocyte function-associated antigen-1. *Anesthesiology* 113, 600-609.
- Yuki, K., Astrof, N.S., Bracken, C., Yoo, R., Silkworth, W., Soriano, S.G., and Shimaoka, M. (2008). The volatile anesthetic isoflurane perturbs conformational activation of integrin LFA-1 by binding to the allosteric regulatory cavity. *FASEB J* 22, 4109-4116.
- Zimmerman, T., Oyarzabal, J., Sebastian, E.S., Majumdar, S., Tejo, B.A., Siahaan, T.J., and Blanco, F.J. (2007). ICAM-1 peptide inhibitors of T-cell adhesion bind to the allosteric site of LFA-1. An NMR characterization. *Chem Biol Drug Des* 70, 347-353.

IntechOpen



## **Magnetic Resonance Spectroscopy**

Edited by Prof. Dong-Hyun Kim

ISBN 978-953-51-0065-2

Hard cover, 264 pages

**Publisher** InTech

**Published online** 02, March, 2012

**Published in print edition** March, 2012

Magnetic Resonance Spectroscopy (MRS) is a unique tool to probe the biochemistry in vivo providing metabolic information non-invasively. Applications using MRS has been found over a broad spectrum in investigating the underlying structures of compounds as well as in determining disease states. In this book, topics of MRS both relevant to the clinic and also those that are beyond the clinical arena are covered. The book consists of two sections. The first section is entitled 'MRS inside the clinic' and is focused on clinical applications of MRS while the second section is entitled 'MRS beyond the clinic' and discusses applications of MRS in other academic fields. Our hope is that through this book, readers can understand the broad applications that NMR and MRS can offer and also that there are enough references to guide the readers for further study in this important topic.

### **How to reference**

In order to correctly reference this scholarly work, feel free to copy and paste the following:

Nathan S. Astrof and Motomu Shimaoka (2012). NMR Spectroscopy for Studying Integrin Antagonists, Magnetic Resonance Spectroscopy, Prof. Dong-Hyun Kim (Ed.), ISBN: 978-953-51-0065-2, InTech, Available from: <http://www.intechopen.com/books/magnetic-resonance-spectroscopy/nmr-spectroscopy-for-studying-integrin-antagonists>

**INTeCH**  
open science | open minds

### **InTech Europe**

University Campus STeP Ri  
Slavka Krautzeka 83/A  
51000 Rijeka, Croatia  
Phone: +385 (51) 770 447  
Fax: +385 (51) 686 166  
[www.intechopen.com](http://www.intechopen.com)

### **InTech China**

Unit 405, Office Block, Hotel Equatorial Shanghai  
No.65, Yan An Road (West), Shanghai, 200040, China  
中国上海市延安西路65号上海国际贵都大饭店办公楼405单元  
Phone: +86-21-62489820  
Fax: +86-21-62489821



© 2012 The Author(s). Licensee IntechOpen. This is an open access article distributed under the terms of the [Creative Commons Attribution 3.0 License](https://creativecommons.org/licenses/by/3.0/), which permits unrestricted use, distribution, and reproduction in any medium, provided the original work is properly cited.

IntechOpen

IntechOpen